Molecular Microbiology (2011) 82(1), 114–130 ■
doi:10.1111/j.1365-2958.2011.07800.x
First published online 30 August 2011

# Inactivation of a novel response regulator is necessary for biofilm formation and host colonization by *Vibrio fischeri*

**Andrew R. Morris, Cynthia L. Darnell and Karen L. Visick***
*Department of Microbiology and Immunology, Loyola University Medical Center, Maywood, IL, USA.*

## Summary

**The marine bacterium *Vibrio fischeri* uses a biofilm to promote colonization of its eukaryotic host *Euprymna scolopes*. This biofilm depends on the symbiosis polysaccharide (*syp*) locus, which is transcriptionally regulated by the RscS–SypG two-component regulatory system. An additional response regulator (RR), SypE, exerts both positive and negative control over biofilm formation. SypE is a novel RR protein, with its three putative domains arranged in a unique configuration: a central phosphorylation receiver (REC) domain flanked by two effector domains with putative enzymatic activities (serine kinase and serine phosphatase). To determine how SypE regulates biofilm formation and host colonization, we generated a library of SypE domain mutants. Our results indicate that the N-terminus inhibits biofilm formation, while the C-terminus plays a positive role. The phosphorylation state of SypE appears to regulate these opposing activities, as disruption of the putative site of phosphorylation results in a protein that constitutively inhibits biofilm formation. Furthermore, SypE restricts host colonization: (i) *sypE* mutants with constitutive inhibitory activity fail to efficiently initiate host colonization and (ii) loss of *sypE* partially alleviates the colonization defect of an *rscS* mutant. We conclude that SypE must be inactivated to promote symbiotic colonization by *V. fischeri*.**

## Introduction

Bacteria possess the ability to adapt and thrive in a wide range of dynamic environments. To establish an ecological niche and prosper within that particular environment, bacteria must be able to sense diverse environmental conditions and then produce the appropriate cellular response. A common mechanism by which bacteria co-ordinate cellular responses with environmental stimuli is via two-component signal transduction (2CST) systems. The typical 2CST system consists of a histidine sensor kinase (SK) and a response regulator (RR). The sensing of an environmental stimulus by the SK initiates a signal transduction cascade by inducing the SK to autophosphorylate at a conserved histidine residue within the transmitter domain (Stock *et al*., 2000; West and Stock, 2001). The phosphoryl group is then transferred from the SK to a downstream RR. RRs catalyse phosphoryl transfer to a conserved aspartate residue located within the N-terminal regulatory receiver (REC) domain (Bourret *et al*., 1990). The phosphorylation state of the REC domain regulates the activity of an attached C-terminal effector domain, often a DNA-binding domain (Stock *et al*., 2000; Gao and Stock, 2010). As a result, RR phosphorylation commonly results in a change in DNA binding and gene expression (reviewed in Galperin, 2010). Alternatively, the RR REC domain may be attached to a large variety of other output domains, including those involved in protein–protein interaction, ligand-binding or enzymatic activity (Galperin, 2006; 2010).

Two-component signal transduction systems are particularly well suited to allow bacteria to sense host signals and then elicit the appropriate response(s) necessary to promote colonization. The marine bacterium *Vibrio fischeri* utilizes multiple 2CST systems to promote symbiotic colonization of its host, the Hawaiian squid *Euprymna scolopes* (Whistler and Ruby, 2003; Bose *et al*., 2007; Hussa *et al*., 2007). In particular, 2CST regulators control one of the earliest stages of host colonization, the formation of a biofilm aggregate on the surface of the squid's symbiotic light organ (Nyholm and McFall-Ngai, 1998; Nyholm *et al*., 2000). The formation of this biofilm depends upon the SK RscS and the RR SypG, which control transcription of the symbiotic polysaccharide locus (*syp*) (Yip *et al*., 2005; 2006; Hussa *et al*., 2008). The current model (Fig. 1) predicts that RscS, upon sensing an as yet unidentified signal, initiates a phosphorelay and donates a phosphoryl group to SypG (Hussa *et al*., 2008). SypG is a *syp*-encoded, $\sigma^{54}$-dependent RR with a DNA-binding output domain (Yip *et al*., 2005). Phosphorylated SypG is thought to directly activate transcription of the *syp*

Accepted 6 August, 2011. *For correspondence. E-mail kvisick@lumc.edu; Tel. (+1) 708 216 0869; Fax (+1) 708 216 9574.

© 2011 Blackwell Publishing Ltd

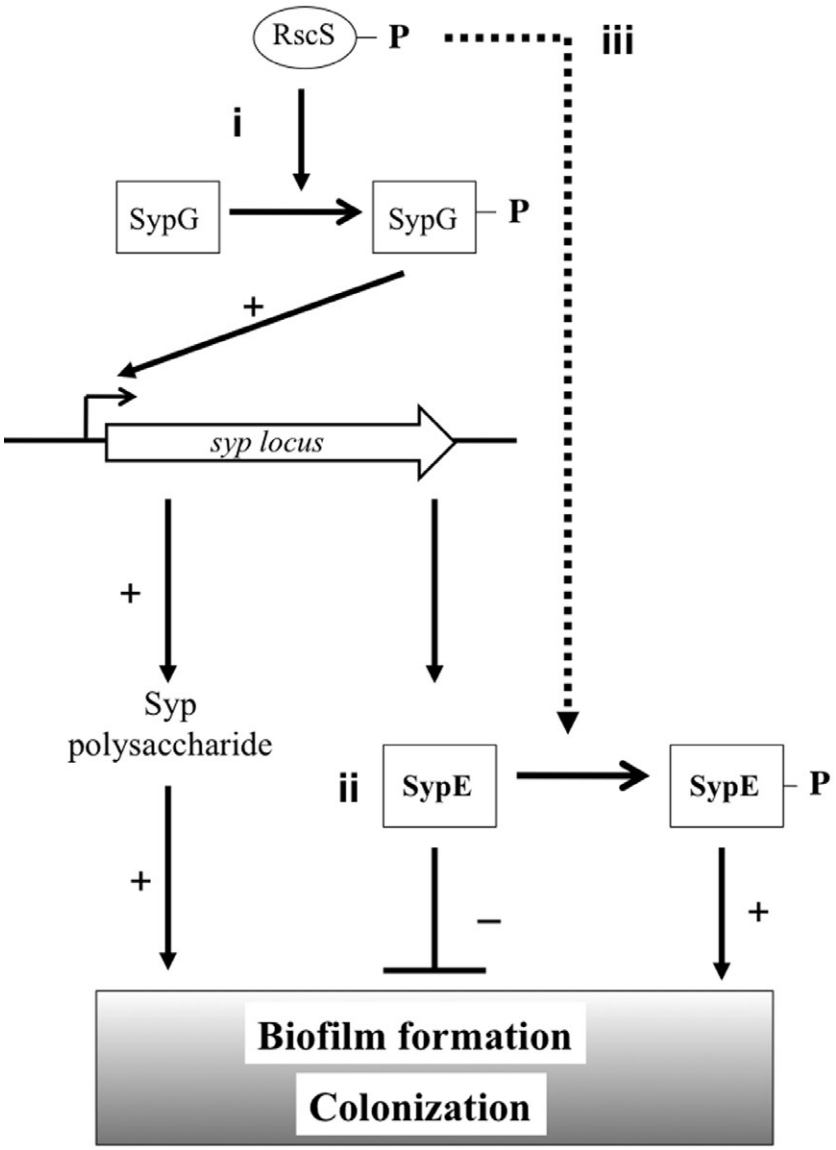


**Fig. 1.** SypE and *syp*-dependent biofilm regulation. Model for the regulation of *syp*-dependent biofilms. (i) Transcription of the *syp* locus is controlled by the RscS–SypG two-component system, which results in expression of the 18 gene *syp* polysaccharide locus and, subsequently, biofilm formation and colonization. (ii) Under non-RscS activating conditions (i.e. upon induction with SypG), SypE functions downstream of *syp* transcription to inhibit biofilm formation. (iii) Upon expression of RscS, SypE inhibitory activity is inactivated, permitting biofilm formation and colonization. Phosphorylation of SypE is predicted to inactivate the inhibitory N-terminal effector domain, while promoting activation of the positive C-terminal effector domain. The dashed arrow indicates potential direct phosphorylation of SypE by RscS, resulting in inactivation of SypE inhibitory activity. (+) denotes positive activity. (–) denotes inhibitory activity.

genes, whose products promote biofilm formation (Hussa *et al*., 2008) (Fig. 1).

Mutant analyses have shown that RscS and SypG are essential both for the formation of *syp*-dependent biofilms and for initiating host colonization (Visick and Skoufos, 2001; Hussa *et al*., 2008). Although the natural signals that activate the *V. fischeri* RscS–SypG system are not yet identified, overexpression of RscS or SypG promotes biofilm formation in laboratory culture and permits a dissection of the pathways leading to this phenotype. Overexpression constructs have been used to investigate the roles of regulatory components in a variety of bacterial systems, including *Vibrio cholerae* and *Salmonella enterica* serovar Typhimurium (Simm *et al*., 2004; Beyhan *et al*., 2006; Shikuma *et al*., 2009). In *V. fischeri*, the multicopy expression of RscS or SypG results in activation of *syp* transcription and the production of robust biofilms. These *syp*-dependent biofilms can be observed by the formation of wrinkled colonies on solid media and pellicle formation at the air–liquid interface in static culture (Yip *et al*., 2005). Importantly, these *in vitro* phenotypes directly correlate with phenotypes observed *in vivo*. In the presence of juvenile squid, induction of the *syp* cluster via multi-copy expression of RscS results in enhanced aggregation on the surface of the host squid's symbiotic light organ, which promotes subsequent colonization events (Yip *et al*., 2006).

In addition to SypG, the *syp* locus encodes a second putative RR, SypE (for a review see Visick, 2009). The SypE protein is unusual both in its structure and in its apparent function in biofilm regulation. Bioinformatic analysis predicts a novel, multi-domain RR with the regu-

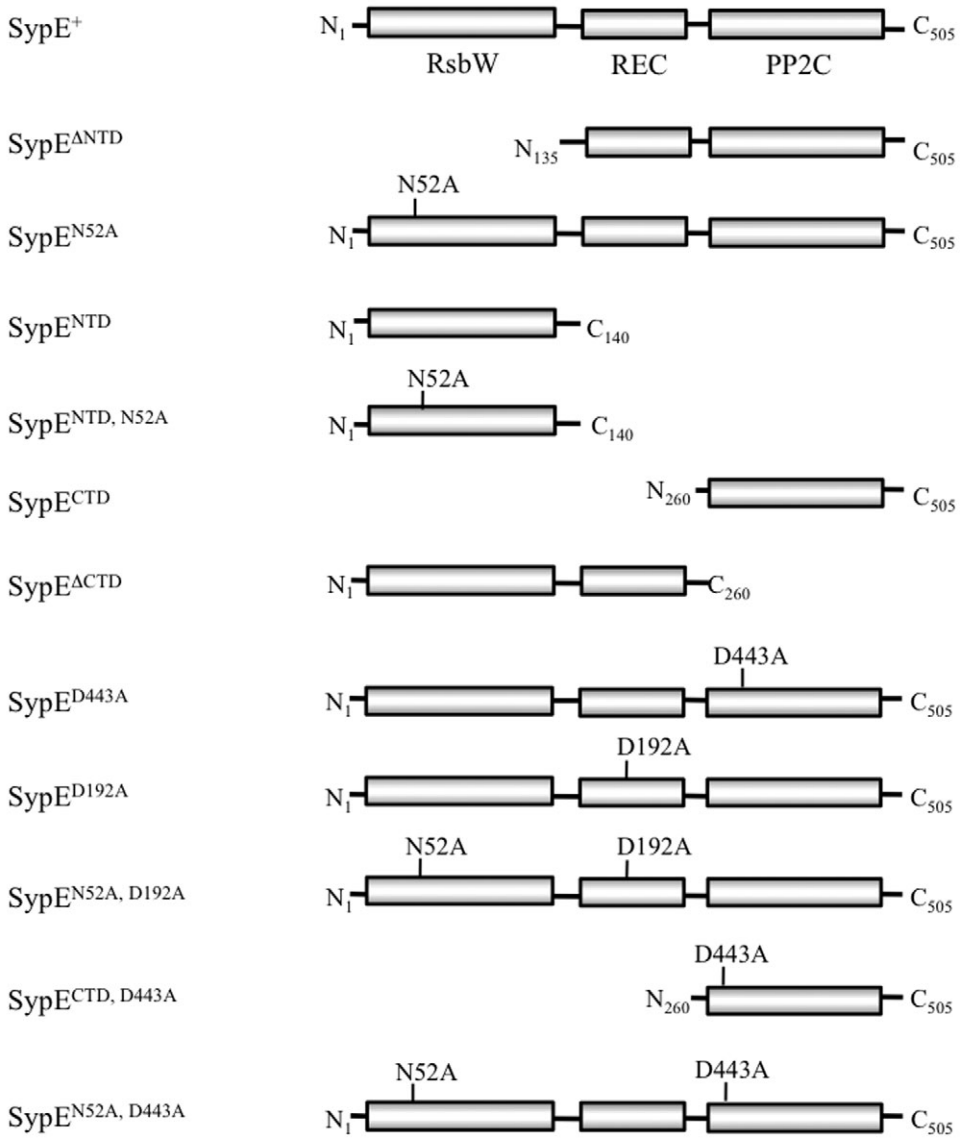


**Fig. 2.** Domain structure of SypE and mutant derivatives. SypE contains a central RR receiver (REC) domain flanked by two putative effector domains, including an N-terminal RsbW-like serine kinase domain and a C-terminal PP2C-like serine phosphatase domain. Conserved residues within the individual domains are indicated (see text for description) (Morris and Visick, 2010). Representations of the various SypE domain mutants generated in this study are presented below. See text for a full description. (Not shown are SypE$^{D495A}$ and SypE$^{CTD,D495A}$.)

latory REC domain in a central position flanked by two terminal effector domains of putative opposing function: an N-terminal RsbW-like serine kinase and a C-terminal PP2C-like serine phosphatase domain (Fig. 2). The presence of a central REC domain flanked by two effector domains of apparent opposing function distinguishes SypE as a novel RR protein.

Previous studies identified SypE as a potential regulator of *V. fischeri* biofilms. Hussa *et al*. (2008) demonstrated that overexpression of the SK RscS in a strain lacking *sypE* resulted in diminished biofilm phenotypes, indicated by a decrease in wrinkled colony formation relative to wild-type cells overexpressing RscS. These results suggested a positive regulatory role for SypE. In contrast, SypE appeared to strongly inhibit biofilms induced by SypG: overexpression of SypG in wild-type cells resulted in smooth colony formation and poor pellicle production, while its overexpression in a Δ*sypE* strain induced robust biofilms similar to that of an RscS-overexpressing wild-type strain. We hypothesize that SypE plays a novel role as a dual regulator of biofilm formation and that these activities must be controlled to permit biofilm formation and colonization (Fig. 1).

Here, we investigated the role of this unusual regulator in the control of biofilm formation and host colonization by *V. fischeri*. We found that the N- and C-terminal domains

of SypE play negative and positive roles, respectively, in the control of biofilm formation. We further determined that the ability of SypE to switch to a biofilm-promoting activity (and away from an inhibitory activity) depends upon residue D192, the predicted site of phosphorylation within the central receiver domain. Finally, we found that the ability of SypE to inhibit biofilm formation *in vitro* correlated with its ability to inhibit host colonization and symbiotic aggregation. Together, our data suggest that inactivation of SypE is a critical step in symbiotic biofilm formation and colonization by *V. fischeri*.

## Results

### *Deletion of* sypE *impairs RscS-induced biofilm phenotypes*

*sypE* encodes an unusual, multi-domain RR protein consisting of a central receiver (REC) domain flanked by N- and C-terminal effector domains with sequence similarity to serine kinases and serine phosphatases respectively (Fig. 2) (Morris and Visick, 2010). Consistent with the complex nature of this protein, SypE appears to both positively and negatively impact biofilm formation by *V. fischeri* (Hussa *et al*., 2008). In this work, our goal was to understand how the individual domains contribute to these opposing regulatory activities, and how these activities are regulated.

Because the natural signal(s) to which RscS responds are not yet known, we overexpressed *rscS* to induce biofilm formation throughout these experiments. As previously discussed, biofilm formation appeared diminished by the deletion of *sypE* (Hussa *et al*., 2008). To better understand this putative role of SypE as a positive regulator, we examined biofilm development over time by wild-type and Δ*sypE* mutant cells containing the RscS-expressing plasmid, pARM7 (pRscS). In addition, to verify that any phenotypes of the Δ*sypE* mutant were due to the loss of *sypE*, and were not the result of a polar effect on downstream genes, we complemented the *sypE* null strain with a wild-type *sypE* allele (*sypE*$^+$) inserted in the chromosome at the Tn*7* integration site. As a control, we inserted an empty Tn*7* cassette (EC) at the same site.

First, we evaluated the formation of wrinkled colonies using a spotted culture technique (*Experimental procedures*). We found that RscS-expressing wild-type cultures consistently began to exhibit wrinkled colony morphology within 14 h of growth, while a *sypE* deletion strain consistently exhibited a 4–6 h delay, initiating wrinkled colony formation around 18–20 h post spotting (Fig. 3A and data not shown). Complementation with *sypE*$^+$ at the Tn*7* site largely restored the timing and pattern of wrinkled colony development. We noted that at a late (48 h) time point, all the strains exhibited a similar degree of wrinkled colony morphology, indicating that deletion of *sypE* only results in a temporal delay in RscS-induced wrinkled colony development. As expected, cells carrying the empty vector (pKV282) never formed wrinkled colonies (Fig. 3A).

Second, we evaluated the production of pellicles over time. When grown statically in HEPES minimal medium (HMM), RscS-expressing wild-type cells produced a structured pellicle at the air–liquid interface within 24 h of incubation, while vector control cells failed to form any observable pellicle (Fig. 3B) (Yip *et al*., 2005). The Δ*sypE* strain formed a diminished RscS-induced pellicle at 24 h that was easily disrupted relative to wild-type control cells (Fig. 3B). Complementation with *sypE*$^+$ restored robust pellicle formation. Attempts to quantify the RscS-induced pellicles using crystal violet staining were not successful, as the crystal violet stained only the glass-attached cell mass and not the overall pellicle (A.R. Morris and K.L. Visick, unpubl. data). Therefore, we utilized confocal microscopy to assess pellicle biofilms produced by wild-type and Δ*sypE* strains overexpressing both *rscS* and green fluorescent protein (GFP) at 24 h post inoculation. RscS-expressing wild-type cells exhibited increased pellicle attachment relative to vector-containing cells, with an average biofilm thickness of 15 (± 2) and 4 (± 1) μm respectively (Fig. 3C). Compared with wild-type cells, the Δ*sypE* mutant strain consistently exhibited a 50% reduction in RscS-induced pellicle attachment with an average biofilm thickness of 8 (± 1) μm (Fig. 3C). Complementation with *sypE*$^+$ increased the average biofilm thickness to 13 (± 1) μm (Fig. 3C). These results confirm that loss of *sypE* impairs the development of biofilm formation, and support the hypothesis that under RscS-overexpressing conditions SypE exerts positive regulatory activity.

### *The SypE C-terminal domain is required for positive regulation of biofilm phenotypes*

To determine the role(s) of the individual SypE domains in the positive regulation of RscS-induced *V. fischeri* biofilms, we constructed a library of SypE domain mutants (Fig. 2). We then assessed the ability of these *sypE* alleles to complement the *sypE* mutant by inserting these constructs into the Tn*7* site of the Δ*sypE* strain and assaying for restoration of RscS-induced biofilm phenotypes (i.e. wrinkled colony morphology and pellicle formation). We performed time-course experiments using these complemented strains, but show here only the appropriate, representative time points.

As previously observed (Fig. 3), RscS-induced wild-type cells exhibited signs of wrinkled colony development within 16 h (Fig. 4A), whereas wild-type cells containing vector control fail to form a biofilm (Fig. 4B). At the early, 16 h time point, the Δ*sypE* strain (Fig. 4C) exhibited a

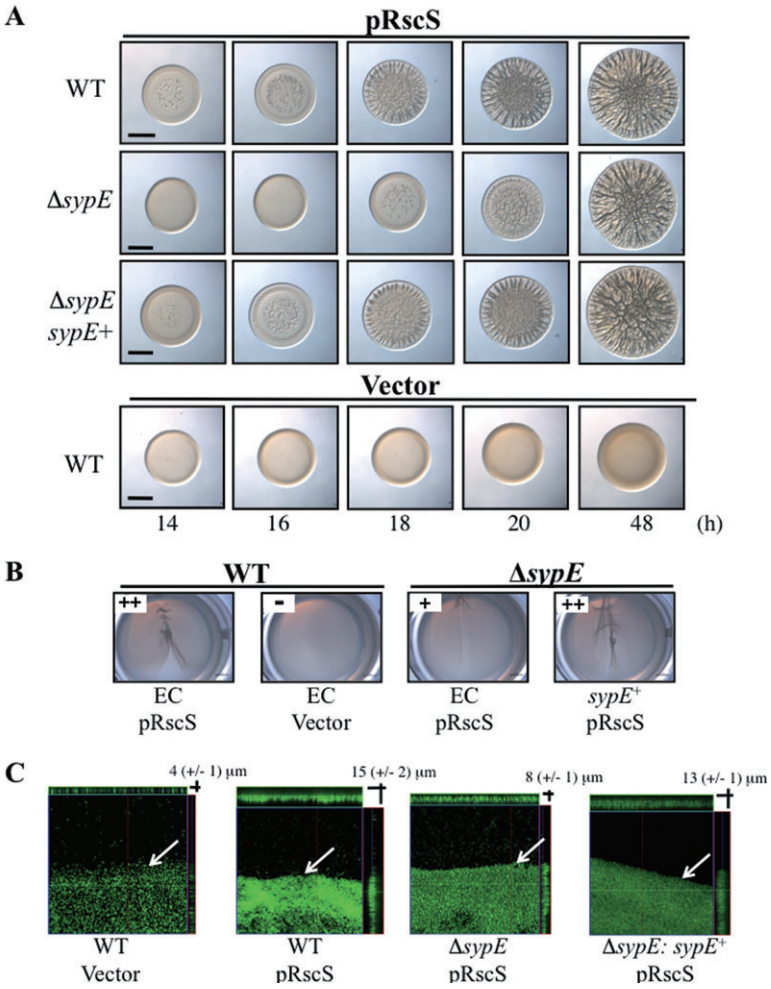


**Fig. 3.** Impact of SypE on RscS-induced biofilm phenotypes.
A. Time-course of RscS-induced wrinkled colony formation. Cultures of the following strains were spotted onto LBS medium at RT and wrinkled colony formation was assessed at various times up to 48 h post spotting: wild-type (WT) cells containing the empty Tn*7* cassette (EC) (KV4389) and carrying pRscS plasmid pARM7 or vector control (pKV282); Δ*sypE* cells carrying pARM7 and either containing EC (KV4390) or complemented with WT *sypE*$^{+}$ (KV4819). Black bar represents 2 mm.
B. Pellicle formation in static culture. Cultures of the following strains were grown in HMM in 24-well plates at RT for 48 h: WT cells containing EC (KV4389) and carrying the vector control pKV282 or pARM7; pARM7-carrying Δ*sypE* containing EC (KV4390) or complemented with *sypE*$^{+}$ (KV4819). A pipette tip was dragged over the surface of the air–liquid interface to visualize the pellicle, and relative pellicle strength was determined as described in *Experimental procedures*.
C. Confocal microscopy of pellicles. The development of RscS-induced pellicle attachment to glass coverslips was visualized via confocal microscopy at 24 h post inoculation. Representative views of the *xy* plane and *z* sections are shown for GFP-labelled derivatives of the strains described in (B). White arrows indicate the air–liquid interface. Photographs are representative of at least three independent experiments.

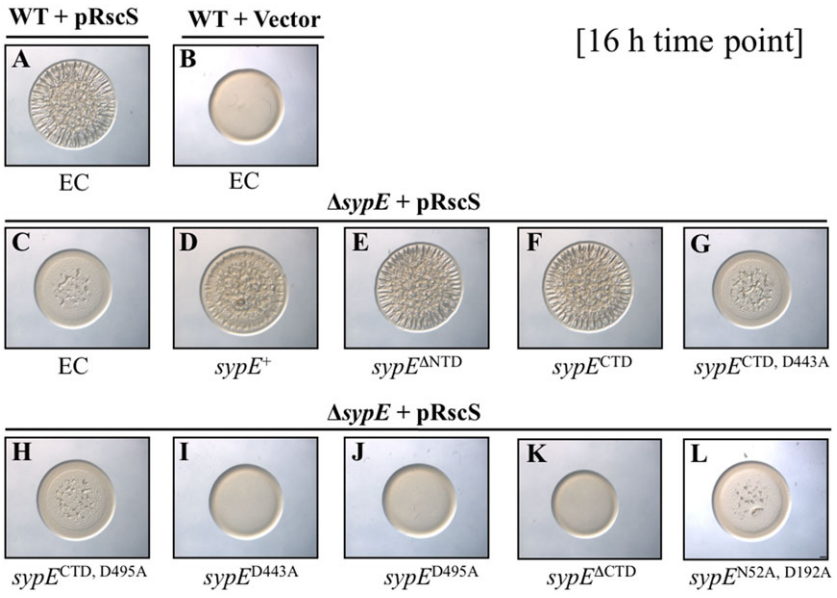


**Fig. 4.** SypE C-terminal domain positively regulates RscS-induced biofilms. Cultures of the following strains were spotted onto LBS medium at RT and wrinkled colony formation was assessed at an early time point (16 h) post spotting: WT cells containing EC (KV4389) and carrying either pRscS plasmid pARM7 (A) or vector control pKV282 (B), and Δ*sypE* mutants carrying pARM7 and containing EC (KV4390) (C) or complemented with WT *sypE*$^{+}$ [KV4819] (D), *sypE*$^{\Delta NTD}$ [KV5124] (E), *sypE*$^{CTD}$ [KV5204] (F), *sypE*$^{CTD,D443A}$ [KV5314] (G), *sypE*$^{CTD,D495A}$ [KV5345] (H), *sypE*$^{D443A}$ [KV4886] (I), *sypE*$^{D495A}$ [KV4887] (J), *sypE*$^{\Delta CTD}$ [KV5315] (K) or *sypE*$^{N52A,D192A}$ [KV5205] (L). Photographs are representative of at least three independent experiments.

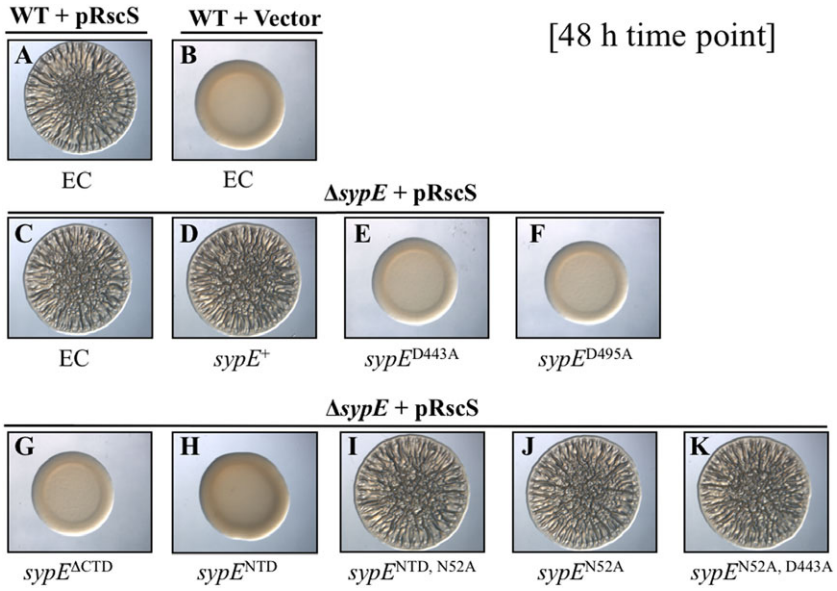


**Fig. 5.** SypE N-terminal domain inhibits RscS-induced biofilms. Cultures of the following strains were spotted onto LBS agar medium at RT and wrinkled colony formation was assessed at a late time point (48 h) post spotting: WT cells containing EC (KV4389) and either pRscS plasmid pARM7 (A) or vector control pKV282 (B); Δ*sypE* cells carrying pARM7 and containing EC (KV4390) (C) or complemented with WT *sypE*$^{+}$ [KV4819] (D), *sypE*$^{D443A}$ [KV4886] (E), *sypE*$^{D495A}$ [KV4887] (F), *sypE*$^{\Delta CTD}$ [KV5315] (G), *sypE*$^{NTD}$ [KV5129] (H), *sypE*$^{NTD,N52A}$ [KV5143] (I), *sypE*$^{N52A}$ [KV5142] (J), *sypE*$^{N52A,D443A}$ [KV5379] (K). Photographs are representative of at least three independent experiments.

delay in RscS-induced wrinkling relative to wild-type cells (Fig. 4A), but this delay could be complemented with a wild-type copy of *sypE*$^{+}$ (Fig. 4D). Similarly, we found that expression of a SypE N-terminal deletion mutant (SypE$^{\Delta NTD}$) (Fig. 2) fully complemented the *sypE* deletion for both wrinkled colony morphology and pellicle formation (Fig. 4E and Fig. S1). This mutant lacks the N-terminal 135 amino acids encoding the putative serine kinase domain but retains an intact C-terminal serine phosphatase domain and REC domain. We conclude from these data that the positive regulatory activity of SypE is retained in this deletion mutant and thus does not require the N-terminal domain.

We hypothesized that the positive regulatory activity retained in the SypE$^{\Delta NTD}$ mutant protein may reside in the C-terminal effector domain. Indeed, a deletion derivative that expresses only the C-terminal 245 amino acids (SypE$^{CTD}$) (Fig. 2) fully complemented the Δ*sypE* deletion, restoring wrinkled colony morphology (Fig. 4F) and pellicle production (Fig. S1) to wild-type levels. We also observed that expression of SypE$^{CTD}$ in the Δ*sypE* mutant was sufficient to restore pellicle attachment to near wild-type levels (16 ± 1 μm) as determined by confocal microscopy (data not shown). These data thus demonstrate that the C-terminal effector domain of SypE alone is active and can positively regulate RscS-induced biofilms.

### *The positive activity of the C-terminal domain of SypE requires conserved aspartates*

The C-terminal effector domain of SypE exhibits weak sequence similarity to serine phosphatases of the PP2C family, including RsbU and SpoIIE of *Bacillus subtilis* (Morris and Visick, 2010). Proteins of the PP2C family are $Mg^{2+}$/$Mn^{2+}$-dependent phosphatases, and possess several invariant aspartate residues required for co-ordination of divalent cation binding and catalytic activity (Adler *et al.*, 1997; Jackson *et al.*, 2003). SypE contains several of these residues, including the conserved aspartates (Asp-443 and Asp-495) (Morris and Visick, 2010). We therefore reasoned that these conserved residues were likely required for the observed positive regulatory activity. We generated alanine substitutions in the context both of the C-terminal domain alone (SypE$^{CTD,D443A}$ and SypE$^{CTD,D495A}$) and of the full-length protein (SypE$^{D443A}$ and SypE$^{D495A}$) (Fig. 2 and not shown). Mutation of either conserved aspartate in the context of the C-terminal domain alone (SypE$^{CTD,D443A}$ and SypE$^{CTD,D495A}$) resulted in failure to complement the Δ*sypE* defect: these mutants exhibited delayed wrinkled colony morphology and pellicle formation similar to the uncomplemented Δ*sypE* control (Fig. 4G and H and Fig. S1). To ensure that both the SypE$^{CTD,D443A}$ and the SypE$^{CTD,D495A}$ proteins were indeed expressed, we FLAG-tagged these proteins and confirmed their expression by Western blot analysis (Fig. S2A). We conclude that the positive regulatory activity of the SypE C-terminal domain requires the conserved aspartate residues (D443 and D495).

In the context of the full-length SypE, the SypE$^{D443A}$ and SypE$^{D495A}$ mutants again failed to complement the *sypE* deletion as observed at the early (16 h) time point (see Fig. 4I and J respectively), but unexpectedly also completely inhibited biofilm formation, as indicated by smooth colony morphology (Fig. 5E and F respectively) and lack of pellicle even at the 48 h time point (Fig. S1). This result was not due to aberrant protein expression, as these proteins were present at levels similar to the wild-type SypE control (Fig. S2B).

We hypothesized that loss of function in SypE's C-terminus 'locked' SypE into an inhibitory state. Consistent with that interpretation, we found that a SypE$^{\Delta CTD}$ mutant, which contains the N-terminus and the central REC domain, but lacks the C-terminal domain, exhibited the same phenotype: this strain failed to form wrinkled colonies and pellicles even at late time points (48 h post incubation) (Figs 4K and 5G and Fig. S1). Taken together, these results demonstrate that an intact C-terminal domain is required for the positive regulatory activity of SypE and that loss of the C-terminal function results in a protein with constitutive inhibitory activity.

### *The N-terminal domain of SypE mediates negative regulation of biofilm phenotypes*

We hypothesized that the inhibitory activity observed upon disruption of the C-terminal domain likely resides in the protein's N-terminal effector domain. To test this hypothesis, we evaluated biofilm formation at a late time point (48 h) in a Δ*sypE* strain that expressed only the 140 amino acids comprising the N-terminal domain (SypE$^{NTD}$). This strain failed to form biofilms, as indicated by the smooth colony morphology and lack of pellicle production at 48 h (Fig. 5H and Fig. S3). These results demonstrate that the isolated SypE N-terminal effector domain is active and sufficient to inhibit the development of RscS-induced biofilm phenotypes.

The N-terminal domain of SypE exhibits sequence similarity to HPK-like serine kinases of the Gyrase, Hsp90, histidine kinase, MutL (GHKL) superfamily, including RsbW of *B. subtilis* (Morris and Visick, 2010). Serine kinases of the GHKL superfamily are demonstrated to form an ATP-binding Bergerat fold consisting of four conserved motifs termed the N, G1, G2 and G3 boxes (Bergerat *et al*., 1997; Dutta and Inouye, 2000). In particular, a conserved asparagine residue located within the N box motif is required for co-ordination of a $Mg^{2+}$ ion involved in ATP binding (Dutta and Inouye, 2000). The N-terminal domain of SypE possesses these conserved ATP-binding residues, including an invariant asparagine residue (N52) (Morris and Visick, 2010) (Fig. 2).

We asked whether the conserved asparagine N52 is required for the inhibitory activity of SypE by substituting alanine at that position. In the context of the inhibitory NTD alone (SypE$^{NTD,N52A}$), this substitution resulted in loss of inhibitory activity: expression of SypE$^{NTD,N52A}$ in the Δ*sypE* strain resulted in delayed wrinkled colony morphology and reduced pellicles similar to empty cassette (EC) control (Fig. 5I and Figs S3 and S4E). Western blot analysis confirmed that the SypE$^{NTD,N52A}$ protein was expressed at levels similar to the SypE$^{NTD}$ control, indicating that the loss of inhibitory activity results from the N52A mutation (Fig. S2A). As expected, the N52A mutation in the context of the full-length protein (SypE$^{N52A}$) permitted complementation of the *sypE* deletion; the SypE$^{N52A}$ strain exhibited wrinkled colony morphology (Fig. 5J and Fig. S4F) and pellicle formation (Fig. S3) similar to the wild-type and *sypE*$^{+}$-complemented strains. These results suggest that the N52A mutation disrupts the inhibitory activity of the SypE protein, but does not impact its positive regulatory activity when a functional C-terminal domain is present.

### *The central REC domain modulates SypE regulatory activity*

Our results demonstrate that SypE exerts both negative and positive control over biofilm formation through the opposing activities of its N- and C-terminal effector domains respectively. In general, the activity of a RR effector domain is regulated by the phosphorylation of a conserved aspartate residue located in the attached REC domain (Stock *et al*., 2000). We therefore hypothesized that the phosphorylation state of the central REC domain likely controls the opposing activities of SypE's terminal effector domains. To test this hypothesis, we evaluated biofilm formation by expressing a SypE mutant containing an alanine substitution at the conserved asparate residue (D192) predicted to be the site of phosphorylation (Hussa *et al*., 2008). This substitution in other RRs results in a protein that cannot become phosphorylated, and whose activity therefore mimics that of the non-phosphorylated state (e.g. Freeman and Bassler, 1999). We found that a SypE$^{D192A}$ mutant not only failed to complement the *sypE* deletion but also completely inhibited wrinkled colony and pellicle formation as observed at the late (48 h) time point (Fig. 6E and Fig. S5). The inhibitory activity of the SypE$^{D192A}$ mutant is not likely due to aberrant protein expression as Western blot analysis indicated that the SypE$^{D192A}$ protein was expressed at levels similar to wild-type SypE (Fig. S2B). These data indicate that the conserved Asp residue (D192) in the REC domain is required for the positive regulatory activity of SypE. Thus, the phosphorylation state of this residue is likely important in controlling SypE regulatory activity.

We hypothesized that the D192A substitution 'locks' SypE into a conformation that favours the inhibitory state. Earlier in this report, we demonstrated that the inhibitory activity of SypE requires an intact N-terminal domain, specifically the conserved residue N52. We predicted that if the D192A mutation 'locks' SypE in a constitutive inhibitory state, then this activity should still require residue N52. To test this, we combined the D192A and N52A mutations (SypE$^{N52A,D192A}$) (Fig. 2). In contrast to the biofilm-inhibitory SypE$^{D192A}$ mutant, cells carrying SypE$^{N52A,D192A}$ exhibited biofilm formation indistinguishable from the uncomplemented (EC) Δ*sypE* control (Fig. 6F and Fig. S5). This result could not be attributed to a defect in protein produc-

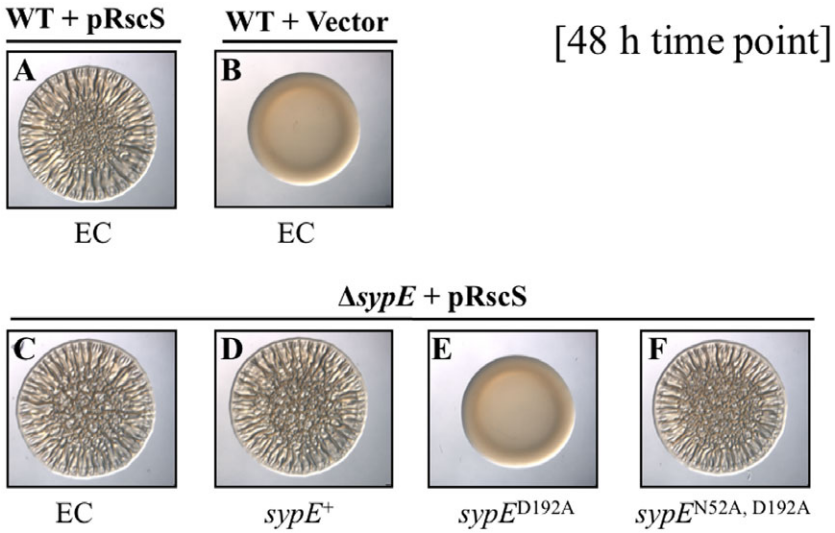


**Fig. 6.** Role of the central REC domain in biofilm regulation. Cultures of the following strains were spotted onto LBS agar medium at RT and wrinkled colony formation was assessed at a late time point (48 h) post spotting: WT cells containing EC (KV4389) and either pRscS plasmid pARM7 (A) or vector control pKV282 (B); and Δ*sypE* mutants carrying pARM7 and containing EC (KV4390) (C) or complemented with WT *sypE*$^{+}$ [KV4819] (D), *sypE*$^{D192A}$ [KV4885] (E), *sypE*$^{N52A,D192A}$ [KV5205] (F). Photographs are representative of at least three independent experiments.

tion of the double mutant (Fig. S2C). These data demonstrate that the N52A mutation is epistatic to the D192A mutation, and that the constitutive inhibitory activity of the D192A mutant requires an intact N-terminal domain. We further noted that while the SypE$^{N52A,D192A}$ mutant lost inhibitory activity, the protein remained incapable of complementing the *sypE* deletion despite the fact that the positive-acting CTD remained intact (Fig. 4L). We conclude from these data that residue D192 is therefore also required for positive regulatory activity. These data suggest that SypE phosphorylation may function both to activate the positive CTD and to inactivate the inhibitory NTD.

We noted that the constitutive inhibitory activity of the SypE$^{D192A}$ mutant mimicked that observed previously in a C-terminal domain mutant, SypE$^{D443A}$. We predicted that the inhibitory activity of the SypE$^{D443A}$ mutant would similarly depend upon residue N52, and tested this by generating a SypE$^{N52A,D443A}$ double mutant (Fig. 2). As expected, a SypE$^{N52A,D443A}$ mutant failed to inhibit biofilm formation, and exhibited delayed wrinkled colony morphology and pellicle formation similar to uncomplemented Δ*sypE* control (Fig. 5K and Figs S3 and S4G). Western blot analysis demonstrated that the SypE$^{N52A,D443A}$ protein was expressed at levels similar to wild-type SypE$^{+}$ (Fig. S2C). These data demonstrate that the N52A mutation is also epistatic to the D443A mutation, and suggest that in all cases SypE inhibitory activity requires an intact N-terminal domain.

### *The negative activity of SypE inhibits host colonization*

Earlier studies demonstrated that the ability to produce *syp*-dependent biofilms is essential for *V. fischeri* cells to efficiently colonize host squid (Visick and Skoufos, 2001; Yip *et al*., 2005; Hussa *et al*., 2007). Because SypE exerts a subtle positive effect and a strong negative effect over biofilm formation, we therefore asked if either or both of these activities were important to host colonization. We evaluated the role of SypE in colonization of juvenile *E. scolopes* using both single-strain inoculations and mixed-strain competitions. We found that deletion of *sypE* did not substantially impact the ability of *V. fischeri* to colonize squid, when in competition or presented alone (Fig. 7A and B respectively), although there was a small advantage for wild-type cells to out-compete the Δ*sypE* mutant [mean log-transformed relative competitive index (Log RCI), $-0.21 \pm 0.63$]. Similar results were also observed when juvenile squid were exposed to a mixture of wild-type and Δ*sypE* cells both overexpressing *rscS*: the squid contained roughly equal numbers of both strains (data not shown). We conclude from these results that loss of *sypE* does not greatly impact colonization fitness. Furthermore, these data suggest that during colonization the minor, positive activity SypE exerts over biofilm formation is not likely critical.

Our *in vitro* studies suggested that, of the two roles of SypE, the inhibitory activity appears to play a more important role with respect to biofilm formation. We therefore asked whether the inhibitory activity of SypE impacts symbiotic colonization. To address this, we focused our attention on the SypE$^{D192A}$ mutant, which exhibits constitutive inhibitory activity. Because *rscS* expressed from the chromosome is active to promote biofilm formation and colonization during symbiotic initiation, we performed these experiments in the absence of *rscS* overexpression. We exposed squid to a mixture of wild-type and Δ*sypE* mutant cells complemented with either wild-type *sypE*$^{+}$ or the inhibitory *sypE*$^{D192A}$ allele. We found that, while the SypE$^{+}$ strain competed well for colonization with the wild-type strain (mean Log RCI,

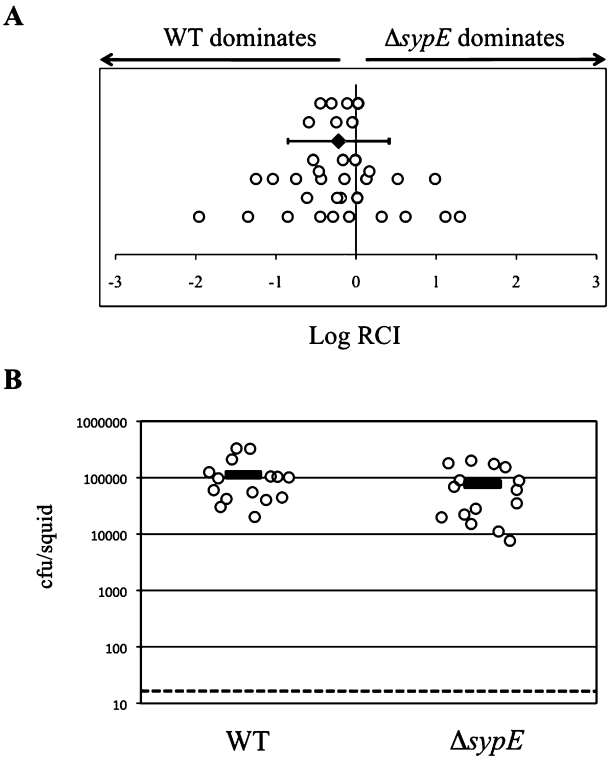


**Fig. 7.** Impact of SypE positive activity on host colonization.
A. Competitive colonization with WT and Δ*sypE* mutant strains. Newly hatched squid were exposed to a mixed inoculum of WT (ES114) and Δ*sypE* cells, in which one strain carried an erythromycin resistance ($Em^R$) marker. Reciprocal experiments in which the other strain carried the $Em^R$ marker were also performed and yielded similar results. The Log relative competitive index (Log RCI) is plotted on the *x*-axis. The log RCI was calculated as the Log ratio of $Em^R$ bacteria in the homogenate divided by the ratio of $Em^R$ bacteria in the inoculum. Each circle represents a single animal ($n = 30$). The position of the circles on the *y*-axis is merely for spacing. The black diamond and error bars indicate the average Log RCI and standard deviation for 30 animals.
B. Single-strain colonization with WT and Δ*sypE* strains. Newly hatched squid were exposed for 18 h to either WT or Δ*sypE* mutant cells. Each circle represents the number of *V. fischeri* cells recovered from an individual animal ($n = 15$). The black bar indicates the average cfu for 15 animals. The data shown in (B) are from one experiment and are representative of at least three independent experiments.

–0.07 ± 0.44), the $SypE^{D192A}$ mutant exhibited a strong colonization defect (mean Log RCI, –1.59 ± 0.52), with all squid colonized predominantly by the wild-type cells (Fig. 8A and B respectively). These data suggested that the inhibitory activity of SypE is detrimental to colonization.

To explore this possibility further, we performed single-strain colonization experiments. Squid inoculated with wild-type cells contained levels of bacteria between $10^4$ and $10^5$ colony-forming units (cfu) per animal, and those inoculated with the Δ*sypE* mutant complemented with wild-type $sypE^+$ were similarly proficient at colonization (Fig. 8C). However, squid inoculated with the Δ*sypE* mutant complemented with $sypE^{D192A}$ exhibited a dramatic defect in host colonization relative to wild-type cells: multiple squid remained completely uncolonized, while the others had a severe decrease in their level of colonization (2–3 log decrease) (Fig. 8C). These data indicate

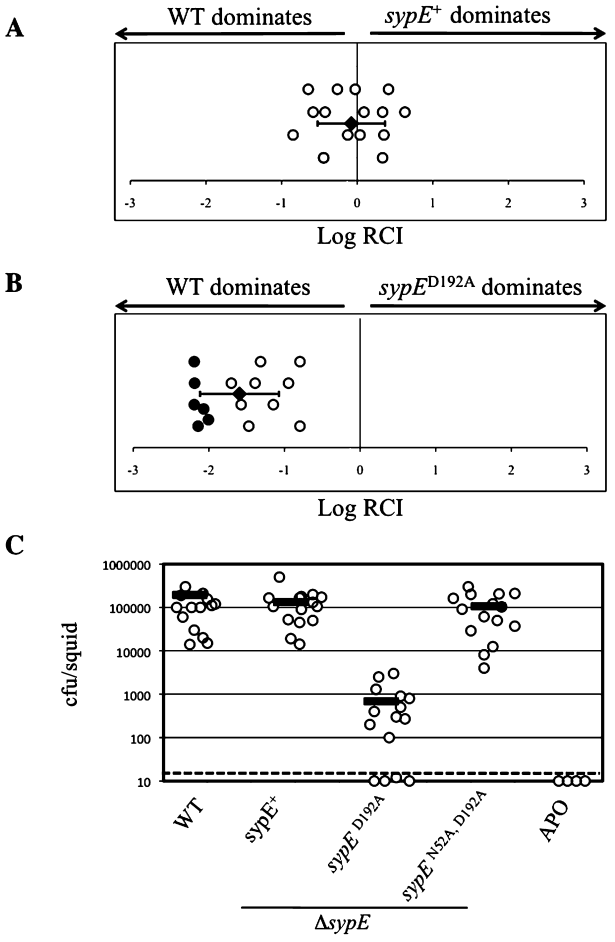


**Fig. 8.** SypE-mediated inhibition of host colonization.
A and B. Competitive colonization with WT and *sypE* mutant strains. Newly hatched squid were exposed to a mixed inoculum of WT (ES114) and Δ*sypE* cells complemented with either WT $sypE^+$ (A) or $sypE^{D192A}$ (B). The Log RCI is plotted on the *x*-axis. The log RCI was calculated as in Fig. 7. The position of the circles on the *y*-axis is merely for spacing. Closed circles indicate squid containing no *sypE* mutant cells. The black diamond and error bars indicate the average Log RCI and standard deviation for 15 animals. Data shown are representative of at least three independent experiments.
C. Single-strain colonization by WT ES114 and *sypE* strains. Newly hatched squid were exposed for 18 h to WT (ES114) or Δ*sypE* strains complemented with either WT $sypE^+$, $sypE^{D192A}$ or the $sypE^{N52A,D192A}$ double mutant. As a negative control, aposymbiotic (APO) juvenile squid were maintained in bacteria free water. Each circle represents the number of *V. fischeri* cells recovered from an individual animal. The dashed line indicates the limit of detection. The black bar indicates the average cfu for 15 animals. The data shown above are from one experiment and are representative of at least three independent experiments.

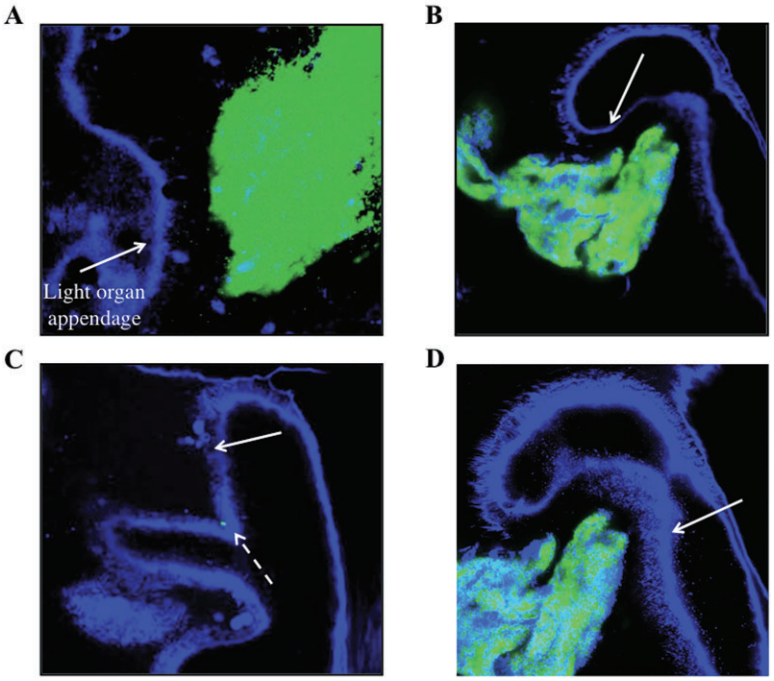


**Fig. 9.** SypE impacts RscS-induced aggregation on the light organ surface. Newly hatched juvenile squid were inoculated with GFP-labelled derivatives of the following strains: (A) pARM7 (pRscS) in WT cells [KV4389] or Δ*sypE* cells complemented with WT *sypE*$^{+}$ [KV4819] (B), *sypE*$^{D192A}$ [KV4885] (C) or *sypE*$^{N52A,D192A}$ [KV5205] (D). After 3 h, animals were stained with CellMask stain (blue colour) and the light organs were examined by confocal microscopy. Representative images of *V. fischeri* cells aggregating on the light organ surface are shown. White arrows indicate the surface of the light organ appendages. The white, dashed arrow indicates single *V. fischeri* cells on the light organ surface.

that residue D192 within the central REC domain, is necessary to promote efficient host colonization.

Finally, to confirm that the colonization disadvantage of the SypE$^{D192A}$ strain is due to the activity of the inhibitory domain, we assessed colonization by the SypE$^{N52A,\ D192A}$-expressing strain. Whereas the SypE$^{D192A}$ mutant inhibited host colonization, the SypE$^{N52A,\ D192A}$ double mutant achieved colonization to near wild-type levels (Fig. 8C). These data support our earlier observations that the inhibitory activity of a SypE$^{D192A}$ mutant resides in the N-terminal effector domain. These results are consistent with the biofilm phenotypes observed in culture, and suggest that the constitutive inhibition of colonization resulting from disruption of the predicted site of phosphorylation (D192) is mediated by the N-terminal effector domain. As such, this inhibitory activity can in turn be disrupted by mutation of the critical N52 site. Together, these data indicate that the inhibitory activity of SypE is physiologically relevant and the ability of the cell to turn off this activity is critical to permit symbiotic colonization.

### *SypE impacts aggregation outside the symbiotic light organ*

*syp*-dependent biofilm formation is required for the initial stages of host colonization, when *V. fischeri* cells aggregate in the squid-secreted mucus on the light organ surface. Previously, Yip *et al*. (2006) reported that *rscS* and *syp* mutants exhibit impaired aggregation and subsequently fail to initiate host colonization, while cells overexpressing *rscS* exhibit enhanced aggregation. To determine if SypE regulates this early stage in symbiotic colonization, we assessed aggregate formation by wild-type or *sypE* mutant strains expressing *rscS* and GFP. In agreement with previous data (Yip *et al*., 2006), wild-type cells exhibited large aggregates (green colour) on the light organ surface (blue colour) (Fig. 9A), as did the Δ*sypE* strain complemented with wild-type *sypE*$^{+}$ (Fig. 9B). In contrast, the SypE$^{D192A}$ mutant strain formed no observable aggregates, with only single cells occasionally observed on the light organ surface (dashed arrow) (Fig. 9C). As expected, the aggregation defect of this mutant was dependent upon the inhibitory N-terminal domain, as a SypE$^{N52A,D192A}$ double mutant formed large aggregates similar to control (SypE$^{+}$) cells (Fig. 9D). These data suggest that the colonization defect of the SypE$^{D192A}$ mutant likely results from a loss of bacterial aggregation at the initiation stage. Thus, SypE appears to impact bacterial aggregation, a critical stage in the initiation of host colonization. Finally, these results support our earlier conclusion that the inhibitory activity of SypE must be deactivated to promote efficient aggregation and host colonization.

### *Deletion of* sypE *improves colonization by an* rscS *mutant*

Our current data demonstrate that the conserved site of phosphorylation in the SypE REC domain is necessary to inactivate the inhibitory activity of the N-terminus and promote its positive activity. Furthermore, although SypE

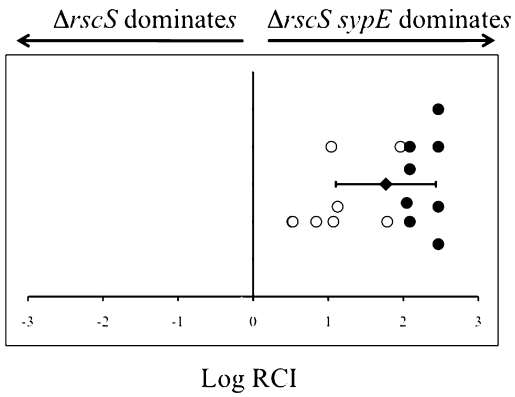


**Fig. 10.** Impact of SypE on host colonization in *rscS* mutant cells. Competitive colonization assay with Δ*rscS* and Δ*rscS* Δ*sypE* mutant cells. Colonization assays were performed and Log RCI of the competing bacterial strains was calculated as described in Fig. 7. Each circle represents a single animal. Closed circles represent animals in which no Δ*rscS* cells were present in the homogenate. The position of the circles on the *y*-axis is merely for spacing. The black diamond and error bars indicate the average Log RCI and standard deviation for 15 animals. The data shown above are from one experiment and are representative of at least three independent experiments.

expressed from its native site in the chromosome inhibits biofilm formation induced by the overexpression of the RR SypG (Hussa *et al*., 2007), it does not inhibit RscS-induced biofilm formation. These data indicate that upon RscS induction, this inhibitory activity of SypE must be turned off. We therefore hypothesized that in a strain lacking *rscS*, SypE is likely to exhibit constitutive inhibitory activity and negatively impact host colonization (Fig. 1). This phenomenon could account, at least in part, for the severe colonization defect of an *rscS* mutant (Visick and Skoufos, 2001). To determine whether this is the case, we generated a Δ*rscS* Δ*sypE* double mutant and assessed the ability of this strain to compete with the Δ*rscS* parent to colonize juvenile squid. Indeed, the Δ*rscS* Δ*sypE* mutant cells dramatically outcompeted the Δ*rscS* single mutant (mean Log RCI, 1.76 ± 0.66) with many animals exclusively colonized by the double mutant (open circles) (Fig. 10). These results indicate that SypE contributes to the colonization defect observed in an *rscS* mutant, supporting our hypothesis and linking SypE-mediated regulation of colonization to the activity of RscS. Together, these data demonstrate that SypE can function as a key regulator of host colonization, restricting colonization to conditions in which RscS is expressed or activated.

## Discussion

In this study, we uncovered a novel and critical role for the RR SypE in the inhibition of biofilm formation and host colonization by *V. fischeri*. Our interest in characterizing SypE was prompted both by its unusual domain architecture and by earlier studies that suggested that SypE regulates *V. fischeri* biofilm regulation (Darnell *et al*., 2008; Hussa *et al*., 2008). Bioinformatics indicate that SypE is a novel RR protein, with its three putative domains arranged in a unique configuration: a central REC domain flanked by two effector domains with apparently opposing activities. We hypothesized that SypE could exert dual regulatory control over *syp* biofilm formation, depending on which of the terminal effector domains was active.

In this report, we performed a genetic analysis of SypE to determine how the individual domains contributed to the protein's apparent dual regulatory activities. We found that SypE indeed possesses both negative and positive regulatory activities that are mediated by the N- and C-terminal effector domains respectively. Although each domain was necessary and sufficient for the respective activities, our data suggested that one domain could influence the activity of another. In particular, we found that mutations within the C-terminal domain not only resulted in loss of SypE positive activity, but also shifted the protein's activity to an inhibitory state. For example, SypE$^{D443A}$ and SypE$^{D495A}$, which were predicted to lack the positive activity and thus behave similar to the uncomplemented (empty cassette) control, instead completely inhibited biofilm formation (Fig. 5E and F). This inhibitory activity depended on an intact N-terminal domain, as a SypE$^{N52A,D443A}$ double mutant lost its inhibitory activity (Fig. 5K). We interpret these data to suggest that the SypE protein structure is sensitive to molecular perturbations. In support of this, we found that the fusion of certain epitope tags to the C-terminus of SypE protein also resulted in aberrant protein activity in which the protein appeared 'locked' in an inhibitory state (A.R. Morris and K.L. Visick, unpubl. data). We speculate that disruption of the C-terminal effector domain likely alters the protein conformation to favour activation of the inhibitory N-terminal domain, perhaps indirectly by impacting phosphorylation of the protein. This would not be unprecedented: mutations within the C-terminal DNA-binding effector domain of the RR OmpR not only affect DNA binding, but also impact the phosphorylation state of the N-terminal REC domain (Tran *et al*., 2000).

Our genetic analysis supports the model that the central REC domain functions to regulate SypE activity. In general, RR activity is controlled through the phosphorylation of a conserved aspartate residue located in the REC domain (Stock *et al*., 2000). REC domains are proposed to exist in an equilibrium of conformational states, which either activate or inactivate an effector domain (Stock and Guhaniyogi, 2006). Phosphorylation of the REC domain is proposed to shift this equilibrium and promote a particular conformational state, resulting in RR activation or inactivation (Stock and Guhaniyogi, 2006).

Our results indicate that an intact REC domain is required to promote the positive regulatory activity of SypE. We found that a SypE mutant that mimics the unphosphorylated state (SypE$^{D192A}$) exhibits constitutive inhibitory activity, thus preventing biofilm formation (Fig. 6E). We interpret these data to indicate that phosphorylation of SypE at residue D192 is required to overcome SypE default inhibitory activity (Fig. 1). In support of this hypothesis, the inhibitory activity of the D192A mutant depended upon an intact N-terminal domain. Furthermore, the loss of inhibitory activity in the SypE$^{N52A,D192A}$ mutant failed to permit the protein to exert its positive activity (see Fig. 4L), suggesting that phosphorylation at residue D192 is still required for activation of the C-terminal domain and, thus, positive activity. Similarly, we found that the conserved aspartate was also required for positive regulatory activity displayed by a SypE mutant lacking the N-terminus (SypE$^{\Delta NTD}$) (A.R. Morris and K.L. Visick, unpubl. data). We propose that REC phosphorylation shifts the equilibrium of the SypE conformational states such that the inhibitory N-terminus is inactivated, while the positively acting C-terminus is activated (Fig. 1).

In our assessment of the SypE REC domain, we attempted to identify mutations that would effectively mimic the phosphorylated state of SypE, resulting in 'constitutively active' SypE and dominant-positive activity. However, we found that several mutations reported to mimic the phosphorylated state in select RRs, such as a SypE$^{D192E}$ (Klose *et al*., 1993) or a SypE$^{D192E,D150K}$ (Bourret *et al*., 1993) mutant, failed to result in the constitutive activation of the positive C-terminal domain (A.R. Morris and K.L. Visick, unpubl. data). The inability of these mutations to result in a SypE mutant that mimics the phosphorylated state is not surprising, as few mutations have been found to universally activate all RRs (Smith *et al*., 2004). Indeed, these common mutations have failed to activate several well-characterized RRs (Bourret *et al*., 1990; Stewart *et al*., 1990; Pazour *et al*., 1992). We hypothesize that, due to the complex domain structure of SypE, these mutations likely fail to mimic the conformational changes induced and/or stabilized by phosphorylation.

An earlier study reported that wild-type SypE inhibited biofilms induced by the RR SypG: overexpression of *sypG* in wild-type cells induced weak biofilm formation, while its overexpression in a Δ*sypE* strain resulted in robust biofilms similar to RscS-induced cells (Hussa *et al*., 2008). In contrast, we have shown here that upon *rscS* overexpression wild-type SypE exhibits positive regulatory activity. These data indicate that while SypG overexpression is capable of inducing *syp* biofilms, it is not sufficient to mimic the natural regulation of SypE and *syp*-dependent biofilms. These data can be explained by a model in which RscS modulates SypE activity (Fig. 1). As such, SypE would promote biofilms under conditions in which RscS is activated, and would prevent aberrant biofilm formation induced under other conditions (such as SypG overexpression). We hypothesize that RscS directs phosphorylation of SypE, as a SypE$^{D192A}$ mutant that cannot become phosphorylated fails to promote biofilm formation (Fig. 6E). Whether RscS can directly phosphorylate SypE, or whether RscS influences the activity of another regulator that acts upon SypE, remains unknown. The possibility that RscS serves as a phosphodonor to both SypG and SypE would not be unprecedented, as other studies have reported a single SK interacting with multiple RRs (e.g. Biondi *et al*., 2006).

In this study, we provide compelling evidence that, in addition to a role in biofilm regulation, SypE also impacts host colonization *in vivo*. Our current data indicate that the minor positive role of SypE in promoting biofilm formation is relatively unimportant, as deletion of *sypE* did not substantially affect host colonization (Fig. 7 and data not shown). It remains possible that the positive activity of SypE does indeed contribute to colonization fitness, but that this impact may not be readily evident given our current experimental conditions. In contrast to the positive activity, we show that inhibition by SypE is a significant activity that must be overcome during the colonization process. We found that cells expressing a SypE mutant disrupted at the predicted site of phosphorylation (SypE$^{D192A}$) exhibited a substantial defect in host colonization (Fig. 8), a defect that could be attributed to the inability of these cells to efficiently aggregate in the squid-derived mucus on the light organ surface, an essential stage in the initiation of host colonization (Fig. 9C). Thus, residue D192 within the central REC domain is absolutely required to inactivate the inhibitory activity of SypE. We propose that phosphorylation at residue D192 is necessary to shift the activity of SypE away from the inhibitory N-terminal domain, and permit activation of the positive C-terminal domain. Consistent with our biofilm results, this inhibition of host colonization and bacterial aggregation by the SypE$^{D192A}$ mutant depended upon an intact N-terminal domain, as cells expressing the SypE$^{N52A,D192A}$ double mutant exhibited near wild-type levels of colonization and aggregation (Figs 8C and 9D). These data underscore the utility of intra-molecular epistasis as a powerful approach to understanding the function of a multi-domain protein.

Together, these results – that (i) SypE inhibitory activity must be inactivated for colonization to proceed, (ii) inactivation of this inhibitory activity depends upon the REC domain and likely phosphorylation at D192, and (iii) the SK RscS promotes this inactivation – permitted us to generate a model for the severe colonization defect observed in an *rscS* mutant (Visick and Skoufos, 2001) (Fig. 1). In this model, RscS would play roles in both inducing *syp* transcription and inactivating the inhibitory activity of SypE. We hypothesized that if this were true, then a Δ*rscS* Δ*sypE*

double mutant should colonize better than an *rscS* mutant. Indeed, we found that the Δ*rscS* Δ*sypE* mutant dramatically outcompeted the Δ*rscS* mutant in competitive colonization assays (Fig. 10). Colonization by the Δ*rscS* Δ*sypE* mutant did not fully mimic that of wild-type cells (A.R. Morris and K.L. Visick, unpubl. data); this is likely due to the additional role of RscS in activating SypG-dependent transcription of the *syp* locus and biofilm formation (Hussa *et al*., 2008). These experiments support the model that the inactivation of SypE inhibitory activity is critical for successful symbiotic colonization. Intriguingly, *sypE* is conserved in the genome of several *syp*-containing vibrios that lack the SK *rscS*, including *V. fischeri* strain MJ11. Previously, Mandel *et al*. (2009) demonstrated that the inability of strain MJ11 to proficiently colonize *E. scolopes* could be attributed to the absence of *rscS*. It is possible that the inhibitory activity of SypE contributes to the inability of MJ11 to colonize *E. scolopes*. A role for SypE in restricting host colonization in *V. fischeri* strain MJ11 or other vibrios awaits future studies.

The mechanism by which SypE controls biofilm formation remains an area of active study. Current evidence indicates that SypE exerts its regulatory control at some unknown level downstream of SypG activation and *syp* transcription (Hussa *et al*., 2008; A.R. Morris and K.L. Visick, unpubl. data). Our genetic and bioinformatic analyses suggest that the N- and C-terminal effector domains likely control biofilm formation through the phosphorylation and dephosphorylation of an as yet unknown downstream target protein. The N- and C-terminal effector domains of SypE share weak sequence similarity to the serine kinase, RsbW, and the serine phosphatase, RsbU, of *B. subtilis* respectively. In *B. subtilis*, these proteins function as regulators of $\sigma^B$ activity in the general stress response pathway (Dufour and Haldenwang, 1994; Voelker *et al*., 1996). In this pathway, both RsbW and RsbU interact with and mediate the phosphorylation and dephosphorylation, respectively, of RsbV, an anti-sigma factor antagonist (Dufour and Haldenwang, 1994; Voelker *et al*., 1996). Intriguingly, the *syp* locus encodes a putative anti-sigma factor antagonist, SypA, which shares sequence similarity to RsbV (Yip *et al*., 2005; Morris and Visick, 2010). Current studies are underway to determine if SypE's effector domains indeed possess serine kinase and serine phosphatase activity, and whether SypA serves as the target of SypE regulatory activity.

We conclude from this study that initiation of host colonization by *V. fischeri* is controlled through the inactivation of a negative regulator. Such a mechanism – inactivation of an inhibitory RR – is rarely observed in other characterized models of colonization. This is also an unusual mechanism for the control of biofilm formation. The data we present here also provide insights into the previously established requirement for the SK RscS in initiating colonization (Visick and Skoufos, 2001) by demonstrating that this regulator is necessary for the inactivation of SypE. That this inactivation is necessary for symbiotic aggregation and colonization, fully correlating with its requirement for biofilms outside the host, further demonstrates the utility of the *V. fischeri*–squid symbiosis as a model for the role of biofilm formation in host colonization. Interestingly, bioinformatic analyses suggest that SypE-like proteins may be present in diverse bacterial species, including vibrios, such as *Aliivibrio salmonicida*, and non-vibrios, such as *Aeromonas veronii*. What function(s), if any, these SypE-like proteins possess in these other organisms remains unknown. Additional characterization of this non-DNA-binding RR with its unusual structure of apparently opposing enzymatic activities will undoubtedly add to our understanding of RR function and diversity, as well as control of biofilm formation and host colonization.

## Experimental procedures

### *Bacterial strains, plasmids and media*

The bacterial strains and plasmids used in this study are listed in Table 1. *V. fischeri* strain ES114, a bacterial isolate from *E. scolopes*, was used as the parental strain in this study (Boettcher and Ruby, 1990). All *V. fischeri* derivatives were generated by conjugation, as previously described (Visick and Skoufos, 2001). The RscS-expressing plasmid, pARM7, was derived from plasmid pKG11 (Yip *et al*., 2006), in which an EcoRI partial digest was performed to remove the chloramphenicol resistance cassette. *Escherichia coli* strains Tam1 *pir* (Active Motif, Carlsbad, CA), DH5α (Invitrogen, Carlsbad, CA) and GT115 (Invivogen, San Diego, CA) were used for cloning and conjugative purposes. *E. coli* strains were grown in Luria–Bertani media (LB) (Davis *et al*., 1980). *V. fischeri* strains were grown in complex media [Sea Water Tryptone (SWT) (Yip *et al*., 2005) or LBS (Graf *et al*., 1994)] or in HMM (Ruby and Nealson, 1977) containing 0.3% Casamino acids and 0.2% glucose (Yip *et al*., 2005). Agar was added to a final concentration of 1.5% for solid media. The following antibiotics were added to *V. fischeri* media, where necessary, at the indicated concentrations: chloramphenicol (Cm) 5 μg ml$^{-1}$ and tetracycline (Tc), 5 μg ml$^{-1}$ in LBS, and 30 μg ml$^{-1}$ in SWT and HMM. The following antibiotics were added to *E. coli* media, where necessary, at the indicated concentrations: Cm at 25 mg ml$^{-1}$, kanamycin (Kan) at 50 μg ml$^{-1}$, Tc at 15 μg ml$^{-1}$ or ampicillin (Ap) at 100 μg ml$^{-1}$.

### *Construction of* sypE *alleles*

The *sypE* alleles used in this study were generated by PCR amplification using the primers listed in Table 2. The PCR products were cloned into the pJET1.2 cloning vector (Fermentas, Glen Burnie, MD), and then subcloned into mobilizable plasmid pVSV105 (Dunn *et al*., 2006) using standard molecular techniques. For chromosomal insertion at the Tn*7* site, the *sypE* genes were subcloned with the upstream $P_{lacZ}$

**Table 1.** Strains and plasmids used in this study

| | Relevant Genotype | Reference |
|---|---|---|
| **Strains** | | |
| *E. coli* | | |
| DH5α | *endA*1 *hsdR17* ($r_K-$ $m_K+$) s*upE*44 thi-1 *recA1 relA* Δ(*lacIZYA-argF*)U169 p*hoA* [ϕ80d*lac*Δ(*lacZ*)M15] | Invitrogen |
| TAM1 λ *pir* | *mcrA* Δ(mrr-hsdRMS-mcrBC) Φ80Δ(*lacz*?M15 Δ*lacX74 recA1 araD139* Δ(*ara-leu*)7697 *galU galK rpsL endA1 nupG* attλ::*pir*+ | Active Motif |
| GT115 | *F- mcrA* Δ*(mrr-hsdRMS-mcrBC)* Φ80*lacz*Δ*M15* Δ*lacX74 recA1 endA1* Δ*dcm uidA(*Δ*MluI)::pir-116* ΔsbcC-sbcD | InvivoGen |
| *V. fischeri* | | |
| ES114 | Wild-type *V. fischeri* | (Boettcher and Ruby, 1990) |
| KV3299 | Δ*sypE* | (Hussa *et al*., 2008) |
| KV4389 | ES114 *att*Tn*7*:: erm | This Study |
| KV4390 | Δ*sypE att*Tn*7*:: erm | This Study |
| KV4819 | Δ*sypE att*Tn*7*:: $P_{lacz}$-*sypE*$^{+}$ (erm) | This Study |
| KV4885 | Δ*sypE att*Tn*7*:: $P_{lacz}$-*sypE*$^{D192A}$ (erm) | This Study |
| KV4886 | Δ*sypE att*Tn*7*:: $P_{lacz}$-*sypE*$^{D443A}$ (erm) | This Study |
| KV4887 | Δ*sypE att*Tn*7*:: $P_{lacz}$-*sypE*$^{D495A}$ (erm) | This Study |
| KV5124 | Δ*sypE att*Tn*7*:: $P_{lacz}$-*sypE*$^{\Delta NTD}$ (erm) | This Study |
| KV5129 | Δ*sypE att*Tn*7*:: $P_{lacz}$-*sypE*$^{NTD}$ (erm) | This Study |
| KV5142 | Δ*sypE att*Tn*7*:: $P_{lacz}$-*sypE*$^{N52A}$ (erm) | This Study |
| KV5143 | Δ*sypE att*Tn*7*:: $P_{lacz}$-*sypE*$^{NTD,\ N52A}$ (erm) | This Study |
| KV5204 | Δ*sypE att*Tn*7*:: $P_{lacz}$-*sypE*$^{CTD}$ (erm) | This Study |
| KV5205 | Δ*sypE att*Tn*7*:: $P_{lacz}$-*sypE*$^{N52A,\ D192A}$ (erm) | This Study |
| KV5314 | Δ*sypE att*Tn*7*:: $P_{lacz}$-*sypE*$^{CTD,\ D443A}$ (erm) | This Study |
| KV5315 | Δ*sypE att*Tn*7*:: $P_{lacz}$-*sypE*$^{\Delta CTD}$ (erm) | This Study |
| KV5345 | Δ*sypE att*Tn*7*:: $P_{lacz}$-*sypE*$^{CTD,\ D495A}$ (erm) | This Study |
| KV5379 | Δ*sypE att*Tn*7*:: $P_{lacz}$-*sypE*$^{N52A,\ D443A}$ (erm) | This Study |
| **Plasmids** | | |
| pARM7 | EcoRI partial digest of pKG11 (*rscS*); tetR | This study |
| pARM47 | pEVS107 containing 1.5 kb *sypE* | This study |
| pARM54 | pEVS107 containing 1.5 Kb *sypE*$^{D192A}$ | This study |
| pARM55 | pEVS107 containing 1.5 Kb *sypE*$^{D443A}$ | This study |
| pARM56 | pEVS107 containing 1.5 Kb *sypE*$^{D495A}$ | This study |
| pARM81 | pEVS107 containing 1.2 Kb *sypE*$^{\Delta NTD}$ | This study |
| pARM82 | pEVS107 containing 700 bp *sypE*$^{CTD}$ | This study |
| pARM89 | pEVS107 containing 500 bp *sypE*$^{NTD}$ | This study |
| pARM90 | pEVS107 containing 1.5 Kb *sypE*$^{N52A}$ | This study |
| pARM91 | pEVS107 containing 500 bp *sypE*$^{NTD,\ N52A}$ | This study |
| pARM101 | pEVS107 containing 1.5 Kb *sypE*$^{N52A,\ D192A}$ | This study |
| pARM109 | pEVS107 containing 700 bp *sypE*$^{CTD,\ D443A}$ | This study |
| pARM110 | pEVS107 containing 1.0 Kb *sypE*$^{\Delta CTD}$ | This study |
| pARM112 | pEVS107 containing 700 bp *sypE*$^{CTD,\ D495A}$ | This study |
| pARM125 | pEVS107 containing 1.5 Kb *sypE*$^{N52A,\ D443A}$ | This study |
| pEVS104 | Conjugal helper plasmid (*tra trb*), KanR | (Stabb and Ruby, 2002) |
| pEVS107 | Mini-Tn7 delivery plasmid; oriR6K, mob; KanR, EmR | (McCann *et al*., 2003) |
| pJET1.2 | Commercial cloning vector; ApR | Fermentas |
| pKV282 | Mobilizable vector; TetR | This Study |
| pVSV105 | Mobilizable vector, R6Kori ori(pES213) RP4 *oriT cat* | (Dunn *et al*., 2006) |

promoter into the mini-Tn*7* delivery vector pEVS107 (McCann *et al*., 2003). The *sypE* alleles were then inserted into the chromosomal Tn*7* site of *V. fischeri* using a tetra-parental mating as previously described (McCann *et al*., 2003). To generate site-directed mutations in *sypE*, we utilized the QuikChange Site-Directed Mutagenesis Kit (Stratagene, La Jolla, CA). Plasmid pCLD48 (Table 1) served as the template for the primer Phos-*lacZ*-up-rev and select *sypE* mutagenic primers (Table 2). Generation of the desired mutations was confirmed by sequence analysis using the Genomics Core Facility at the Center for Genetic Medicine at Northwestern University (Chicago, IL) and ACGT (Wheeling, IL). FLAG epitope fusions to C-terminus of full-length SypE proteins were generated by standard PCR using the forward primer, SypE-F, and reverse primer, SypE-Full-R FLAG (Table 2). FLAG epitope fusions were generated to the C-terminus of the SypE$^{NTD}$ protein using the primers forward primer SypE-F and the reverse primer SypE-RsbW-R FLAG (Table 2). Forward primer, SypE$^{CTD}$-F, and reverse primer, SypE-Full-R FLAG, were used to generate FLAG fusions to the C-terminus of the SypE$^{CTD}$ proteins (Table 2).

### *Wrinkled colony assays*

To observe wrinkled colony formation, strains were streaked onto LBS agar plates containing Tc. Single colonies were

**Table 2.** Primers used in this study.

| Primer name | Sequence (5′–3′) |
|---|---|
| SypE-F | GTCCAAAGAAACCGATTTTTATC |
| SypE-R | TTTTTCTGCACTTATTGATTCTCAATTAACAGC |
| SypE$^{\Delta NTD}$-F | GTGGTGTAATCATGGAGCGTTCCCCTTCCCAT |
| SypE$^{NTD}$-R | CTTAATGGGAAGGGGAACGCTC |
| SypE$^{CTD}$-F | GTGGTGTAATCATGGCCCATACTCTATTACCACAA |
| SypE$^{N52A}$ | TCTGAATGGAGCACCGCTCTAGTTTTGCACCCT |
| SypE$^{D443A}$ | TTAGCATTATTTACTGCTGGGTTATTTGAATCA |
| SypE$^{D495A}$ | GGGACACCACCCAATGCCGATGCATTATTGCTG |
| SypE$^{D192A}$ | GATTTAATTATCTCAGCTATTCAAATGCCTGAA |
| SypE$^{D192E}$ | GATTTAATTATCTCAGAGATTCAAATGCCTGAA |
| SypE-Full-R FLAG | ACCCGGGTTATTTATCATCATCATCTTTATAATCTTGATTCTCAATTAACAG |
| SypE-RsbW-R FLAG | ACCCGGGTTATTTATCATCATCATCTTTATAATCATGGGAAGGGGAACGCTC |
| Phospho-lacZ-R | CCTGTGTGAAATTGTTATCCG |

then cultured with shaking in LBS broth with Tc overnight at 28°C and then subcultured to an $OD_{600}$ of 0.1 in 5 ml of fresh medium. Cells were spun down, washed twice in 70% artificial seawater (ASW) (280 mM $MgSO_4$, 56 mM $CaCl_2$, 1.68 M NaCl, 56 mM KCl), and resuspended in 70% ASW and diluted to an OD of 0.1. Ten microlitres of resuspended cultures were spotted onto LBS agar plates and grown for 48 h at 22°C. Images of the spotted cultures were acquired at the indicated time points using the Zeiss stemi 2000-C dissecting microscope. For RscS-induced wrinkling time-course assays, spot development was followed over a course of 48 h and images taken at indicated time points.

### *Pellicle assay*

Strains were grown with shaking in HMM with Tc at 28°C overnight and then subcultured to an OD of 0.1 in 1.5 ml of fresh medium in 24-well microtitre dishes. Cultures were then grown at room temperature for up to 48 h. The strength of each pellicle was evaluated by disrupting the air–liquid interface with a sterile pipette tip after 48 h of incubation. A pellicle is observed as a disruption at the culture surface. Cultures with no pellicle were scored as (–); cultures with an intermediate/weak pellicle were scored as (+); cultures with a strong pellicle that was able to be lifted from the culture intact were scored as (++).

### *Confocal microscopy*

Cells expressing GFP were grown statically in HMM containing Tc in 12-well microtitre plates with glass coverslips partially submerged into the culture medium. Coverslips were incubated with bacteria at room temperature for 24 h and removed for biofilm examination. A Zeiss LSM 510 confocal microscope (40× objective) was used to collect *xy* plane and *z* sections (*xz* and *yz* plane) images of the biofilms. Representative images were prepared using the Zeiss LSM Image Browser software.

### *Squid colonization assays*

To perform single-strain colonization assays, juvenile squid were placed into ASW (Instant Ocean; Aquarium Systems, Mentor, OH) containing roughly 1000–1500 cells per ml of seawater. Colonization assays were allowed to proceed for 16 h post inoculation, at which time the animals were washed twice in ASW and homogenized to release the light organ contents. Serial dilutions of the light organs were plated and cfu calculated. For competitive colonization assays, juvenile squid were placed into ASW containing approximately 1000 *V. fischeri* cells per ml of seawater. Juvenile squid were inoculated with an approximate 1:1 ratio of mutant and wild-type cells, and colonization was allowed to proceed for 18 h. For these assays, *sypE*$^{+}$ cells were marked with an erythromycin resistance ($Em^R$) cassette within the chromosome at the Tn*7* site. Reciprocal experiments were also performed in which Δ*sypE* cells contained the $Em^R$ marker. The ratio of bacterial strains within the light organs of the animals was assessed through luminescence and homogenization/plating assays as described previously (Yip *et al.*, 2006). The competitive colonization data are reported as the Log RCI. This index is generated by dividing the ratio of mutant to wild type in the homogenate by the ratio present in the inoculum and calculating the $\log_{10}$ value of that number.

### *Symbiont aggregation assays*

Log-phase cells ($OD_{600}$ 0.3–0.6) were grown in 2 ml of SWT medium at 22°C. Bacterial cells were then inoculated into filtered ASW at a concentration of $10^6$ cells per ml. Juvenile squid were then placed into inoculated seawater and the two organisms were allowed to associate at room temperature for 3 h prior to dissection. The juvenile squid were removed to vials containing 2 ml filter-sterilized seawater and 5 μM of the counter-stain, CellMask (Invitrogen, Eugene, OR). The animals were then anaesthetized in filtered ASW containing 2% ethanol. Each squid was placed ventral side up on a depression well slide and dissected to remove the mantle and funnel and expose the light organ. Fluorescently labelled light organs (blue) and GFP-labelled (green) bacteria were viewed using a Zeiss LSM 510 confocal microscope.

### *SypE FLAG protein expression*

FLAG epitope fusions were generated to the C-terminus of wild-type *sypE* or mutant *sypE* derivatives as described

earlier. FLAG-*sypE* alleles were cloned into the expression vector pVSV105 and subsequently conjugated into Δ*sypE* cells containing the *rscS* expressing plasmid (pARM7). Biofilm assays were performed to confirm that the FLAG epitope fusions did not disrupt SypE regulatory activity. Strains were cultured in LBS containing Tc and Cm for 18 h at 28°C and subsequently subcultured to an $OD_{600}$ of 0.2. Two hundred and fifty microlitres of culture was pelleted by centrifugation, lysed in 250 µl of 4× SDS sample buffer and resolved on 10–15% SDS-PAGE gels. Duplicate gels were stained with Coomassie Brilliant Blue in order to ensure roughly equal loading of protein samples. Protein transfer to PVDF membrane was performed using standard Tris-Glycine transfer buffer containing 20% methanol. Western blotting was performed using standard protocols with rabbit anti-FLAG primary antibody and donkey anti-rabbit secondary antibody conjugated to horseradish peroxidase. Blots were imaged by chemiluminescent detection (SuperSignal West Pico Chemiluminescent Substrate, Pierce Biotechnology, Rockford, IL).

## Acknowledgements

We thank Ned Ruby and Margaret McFall-Ngai for the use of *E. scolopes* juveniles and a confocal microscope, and Elizabeth Heath-Heckman and Valerie Ray for assistance in the bacterial aggregation assays. We also thank Alan Wolfe, Jonathan Visick, and members of the Visick and Wolfe labs for critical reading of the manuscript. This work was supported by NIH Grant GM59690 awarded to K.L.V. and a grant from the Conservation Medicine Center of Chicago awarded to A.R.M.

## References

Adler, E., Donella-Deana, A., Arigoni, F., Pinna, L.A., and Stragler, P. (1997) Structural relationship between a bacterial developmental protein and eukaryotic PP2C protein phosphatases. *Mol Microbiol* **23:** 57–62.

Bergerat, A., de Massy, B., Gadelle, D., Varoutas, P.C., Nicolas, A., and Forterre, P. (1997) An atypical topoisomerase II from Archaea with implications for meiotic recombination. *Nature* **386:** 414–417.

Beyhan, S., Tischler, A.D., Camilli, A., and Yildiz, F.H. (2006) Transcriptome and phenotypic responses of *Vibrio cholerae* to increased cyclic di-GMP level. *J Bacteriol* **188:** 3600–3613.

Biondi, E.G., Reisinger, S.J., Skerker, J.M., Arif, M., Perchuk, B.S., Ryan, K.R., and Laub, M.T. (2006) Regulation of the bacterial cell cycle by an integrated genetic circuit. *Nature* **444:** 899–904.

Boettcher, K.J., and Ruby, E.G. (1990) Depressed light emission by symbiotic *Vibrio fischeri* of the sepiolid squid *Euprymna scolopes*. *J Bacteriol* **172:** 3701–3706.

Bose, J.L., Kim, U., Bartkowski, W., Gunsalus, R.P., Overley, A.M., Lyell, N.L., *et al*. (2007) Bioluminescence in *Vibrio fischeri* is controlled by the redox-responsive regulator ArcA. *Mol Microbiol* **65:** 538–553.

Bourret, R.B., Hess, J.F., and Simon, M.I. (1990) Conserved aspartate residues and phosphorylation in signal transduction by the chemotaxis protein CheY. *Proc Natl Acad Sci USA* **87:** 41–45.

Bourret, R.B., Drake, S.K., Chervitz, S.A., Simon, M.I., and Falke, J.J. (1993) Activation of the phosphosignaling protein CheY. II. Analysis of activated mutants by 19F NMR and protein engineering. *J Biol Chem* **268:** 13089–13096.

Darnell, C.L., Hussa, E.A., and Visick, K.L. (2008) The putative hybrid sensor kinase SypF coordinates biofilm formation in *Vibrio fischeri* by acting upstream of two response regulators, SypG and VpsR. *J Bacteriol* **190:** 4941–4950.

Davis, R.W., Botstein, D., and Roth, J.R. (1980) *Advanced Bacterial Genetics*. Cold Spring Harbor, NY: Cold Spring Harbor Laboratory.

Dufour, A., and Haldenwang, W.G. (1994) Interactions between a *Bacillus subtilis* anti-sigma factor (RsbW) and its antagonist (RsbV). *J Bacteriol* **176:** 1813–1820.

Dunn, A.K., Millikan, D.S., Adin, D.M., Bose, J.L., and Stabb, E.V. (2006) New rfp- and pES213-derived tools for analyzing symbiotic *Vibrio fischeri* reveal patterns of infection and lux expression *in situ*. *Appl Environ Microbiol* **72:** 802–810.

Dutta, R., and Inouye, M. (2000) GHKL, an emergent ATPase/kinase superfamily. *Trends Biochem Sci* **25:** 24–28.

Freeman, J.A., and Bassler, B.L. (1999) A genetic analysis of the function of LuxO, a two-component response regulator involved in quorum sensing in *Vibrio harveyi*. *Mol Microbiol* **31:** 665–677.

Galperin, M.Y. (2006) Structural classification of bacterial response regulators: diversity of output domains and domain combinations. *J Bacteriol* **188:** 4169–4182.

Galperin, M.Y. (2010) Diversity of structure and function of response regulator output domains. *Curr Opin Microbiol* **13:** 150–159.

Gao, R., and Stock, A.M. (2010) Molecular strategies for phosphorylation-mediated regulation of response regulator activity. *Curr Opin Microbiol* **13:** 160–167.

Graf, J., Dunlap, P.V., and Ruby, E.G. (1994) Effect of transposon-induced motility mutations on colonization of the host light organ by *Vibrio fischeri*. *J Bacteriol* **176:** 6986–6991.

Hussa, E.A., O'Shea, T.M., Darnell, C.L., Ruby, E.G., and Visick, K.L. (2007) Two-component response regulators of *Vibrio fischeri*: identification, mutagenesis, and characterization. *J Bacteriol* **189:** 5825–5838.

Hussa, E.A., Darnell, C.L., and Visick, K.L. (2008) RscS functions upstream of SypG to control the syp locus and biofilm formation in *Vibrio fischeri*. *J Bacteriol* **190:** 4576–4583.

Jackson, M.D., Fjeld, C.C., and Denu, J.M. (2003) Probing the function of conserved residues in the serine/threonine phosphatase PP2Calpha. *Biochemistry* **42:** 8513–8521.

Klose, K.E., Weiss, D.S., and Kustu, S. (1993) Glutamate at the site of phosphorylation of nitrogen-regulatory protein NTRC mimics aspartyl-phosphate and activates the protein. *J Mol Biol* **232:** 67–78.

McCann, J., Stabb, E.V., Millikan, D.S., and Ruby, E.G. (2003) Population dynamics of *Vibrio fischeri* during infection of *Euprymna scolopes*. *Appl Environ Microbiol* **69:** 5928–5934.

Mandel, M.J., Wollenberg, M.S., Stabb, E.V., Visick, K.L., and Ruby, E.G. (2009) A single regulatory gene is sufficient to alter bacterial host range. *Nature* **458:** 215–218.

Morris, A.R., and Visick, K.L. (2010) Control of biofilm forma-

tion and colonization in *Vibrio fischeri*: a role for partner switching? *Environ Microbiol* **12:** 2051–2059.
Nyholm, S.V., and McFall-Ngai, M.J. (1998) Sampling the light-organ microenvironment of *Euprymna scolopes*: description of a population of host cells in association with the bacterial symbiont *Vibrio fischeri*. *Biol Bull* **195:** 89–97.
Nyholm, S.V., Stabb, E.V., Ruby, E.G., and McFall-Ngai, M.J. (2000) Establishment of an animal–bacterial association: recruiting symbiotic *vibrios* from the environment. *Proc Natl Acad Sci USA* **97:** 10231–10235.
Pazour, G.J., Ta, C.N., and Das, A. (1992) Constitutive mutations of *Agrobacterium tumefaciens* transcriptional activator virG. *J Bacteriol* **174:** 4169–4174.
Ruby, E.G., and Nealson, K.H. (1977) Pyruvate production and excretion by the luminous marine bacteria. *Appl Environ Microbiol* **34:** 164–169.
Shikuma, N.J., Fong, J.C., Odell, L.S., Perchuk, B.S., Laub, M.T., and Yildiz, F.H. (2009) Overexpression of VpsS, a hybrid sensor kinase, enhances biofilm formation in *Vibrio cholerae*. *J Bacteriol* **191:** 5147–5158.
Simm, R., Morr, M., Kader, A., Nimtz, M., and Romling, U. (2004) GGDEF and EAL domains inversely regulate cyclic di-GMP levels and transition from sessility to motility. *Mol Microbiol* **53:** 1123–1134.
Smith, J.G., Latiolais, J.A., Guanga, G.P., Pennington, J.D., Silversmith, R.E., and Bourret, R.B. (2004) A search for amino acid substitutions that universally activate response regulators. *Mol Microbiol* **51:** 887–901.
Stabb, E.V., and Ruby, E.G. (2002) RP4-based plasmids for conjugation between *Escherichia coli* and members of the *Vibrionaceae*. *Methods Enzymol* **358:** 413–426.
Stewart, R.C., Roth, A.F., and Dahlquist, F.W. (1990) Mutations that affect control of the methylesterase activity of CheB, a component of the chemotaxis adaptation system in *Escherichia coli*. *J Bacteriol* **172:** 3388–3399.
Stock, A.M., and Guhaniyogi, J. (2006) A new perspective on response regulator activation. *J Bacteriol* **188:** 7328–7330.
Stock, A.M., Robinson, V.L., and Goudreau, P.N. (2000) Two-component signal transduction. *Annu Rev Biochem* **69:** 183–215.
Tran, V.K., Oropeza, R., and Kenney, L.J. (2000) A single amino acid substitution in the C terminus of OmpR alters DNA recognition and phosphorylation. *J Mol Biol* **299:** 1257–1270.
Visick, K.L. (2009) An intricate network of regulators controls biofilm formation and colonization by *Vibrio fischeri*. *Mol Microbiol* **74:** 782–789.
Visick, K.L., and Skoufos, L.M. (2001) Two-component sensor required for normal symbiotic colonization of *Euprymna scolopes* by *Vibrio fischeri*. *J Bacteriol* **183:** 835–842.
Voelker, U., Voelker, A., and Haldenwang, W.G. (1996) Reactivation of the *Bacillus subtilis* anti-sigma B antagonist, RsbV, by stress- or starvation-induced phosphatase activities. *J Bacteriol* **178:** 5456–5463.
West, A.H., and Stock, A.M. (2001) Histidine kinases and response regulator proteins in two-component signaling systems. *Trends Biochem Sci* **26:** 369–376.
Whistler, C.A., and Ruby, E.G. (2003) GacA regulates symbiotic colonization traits of *Vibrio fischeri* and facilitates a beneficial association with an animal host. *J Bacteriol* **185:** 7202–7212.
Yip, E.S., Grublesky, B.T., Hussa, E.A., and Visick, K.L. (2005) A novel, conserved cluster of genes promotes symbiotic colonization and sigma-dependent biofilm formation by *Vibrio fischeri*. *Mol Microbiol* **57:** 1485–1498.
Yip, E.S., Geszvain, K., DeLoney-Marino, C.R., and Visick, K.L. (2006) The symbiosis regulator *rscS* controls the *syp* gene locus, biofilm formation and symbiotic aggregation by *Vibrio fischeri*. *Mol Microbiol* **62:** 1586–1600.

## Supporting information

Additional supporting information may be found in the online version of this article.

Please note: Wiley-Blackwell are not responsible for the content or functionality of any supporting materials supplied by the authors. Any queries (other than missing material) should be directed to the corresponding author for the article.

**Supplemental Information**

# Inactivation of a novel response regulator is necessary for biofilm formation and host colonization by *Vibrio fischeri*

Andrew R. Morris, Cynthia L. Darnell and Karen L. Visick*

Department of Microbiology and Immunology

Loyola University Medical Center

Maywood, IL

***Corresponding author**
Mailing address:
Karen L. Visick
2160 S. First Ave. Bldg. 105
Department of Microbiology and Immunology
Loyola University Medical Center
Maywood, IL 60153
(708)216-0869
kvisick@lumc.edu

# Morris *et al.*, Supplemental Figure 1

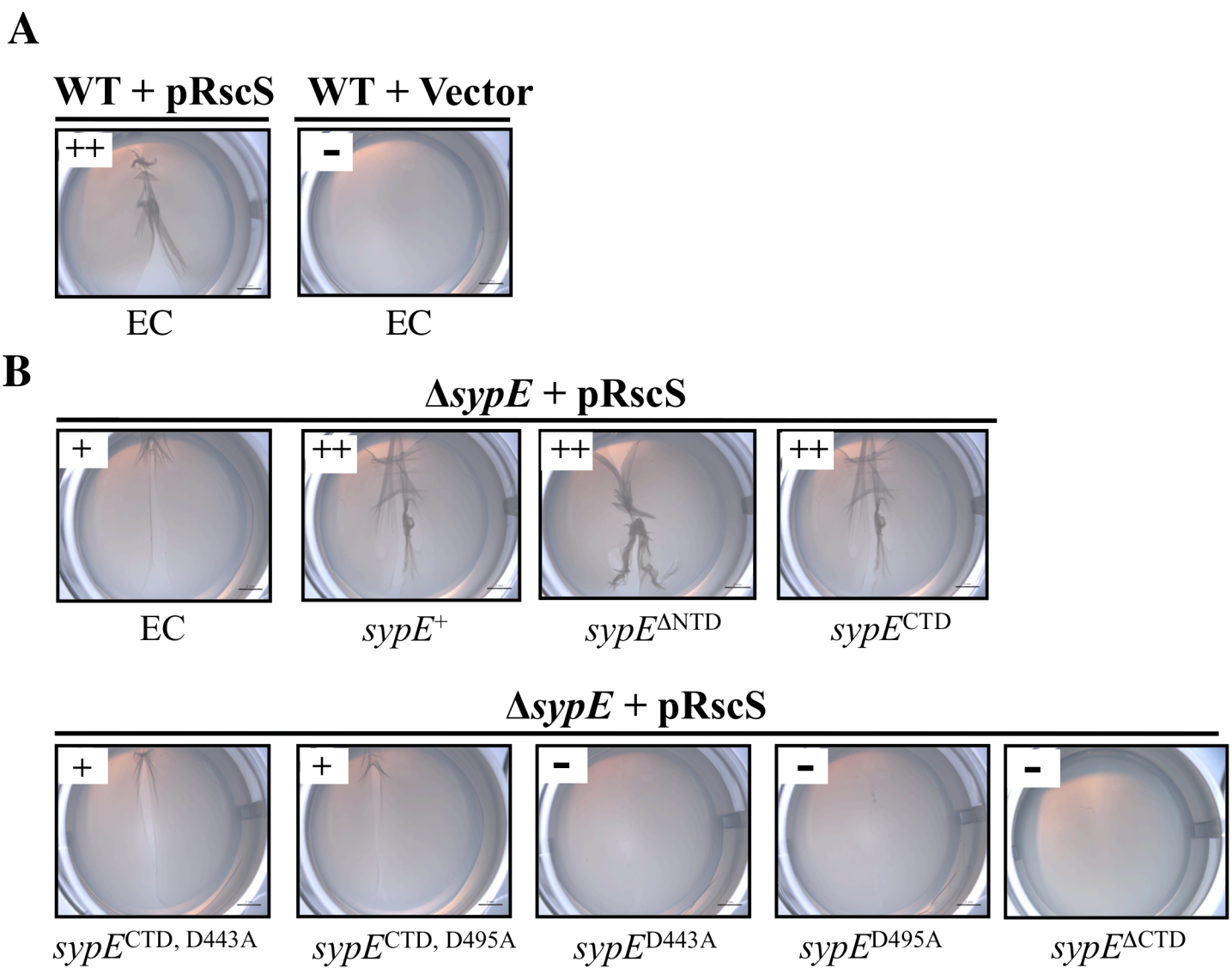


**Supplemental Figure 1. SypE C-terminus promotes RscS-induced pellicle formation**. Pellicle formation assay of RscS-expressing strains. Strains were cultured in HMM at RT and pellicle formation assessed at 48 h post inoculation. (A) Wild-type cells containing empty Tn*7* cassette (EC) and carrying either pRscS plasmid (pARM7) or vector control (pKV282). (B) pARM7 in Δ*sypE* cells complemented with: empty cassette (EC) [KV4390], WT *sypE*$^{+}$ [KV4819], *sypE*$^{\Delta NTD}$ [KV5124], *sypE*$^{CTD}$ [KV5204], *sypE*$^{CTD,\ D443A}$ [KV5314], *sypE*$^{CTD,\ D495A}$ [KV5345], *sypE*$^{D443A}$ [KV4886], *sypE*$^{D495A}$ [KV4887], *sypE*$^{\Delta CTD}$ [KV5315]. A pipette tip was dragged over the surface of the air-liquid interface to visualize the pellicle. The pellicle can be observed as a disturbance at the surface of the culture. (-) denotes no observable pellicle observed upon disturbance with the pipette tip. (+) indicates an intermediate/ weak pellicle that could be easily disrupted by the pipette tip . (++) denotes a strong pellicle that could be lifted from the culture surface.

# Morris *et al*., Supplemental Figure 2

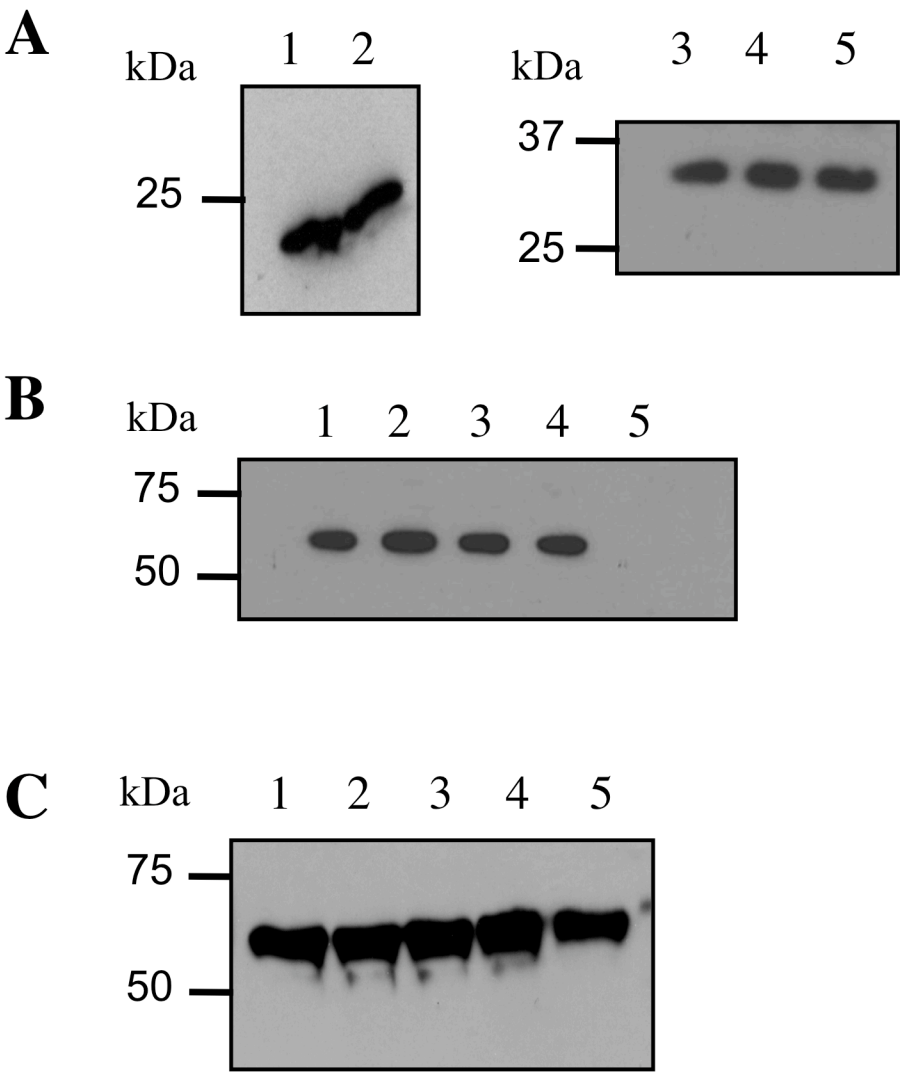


**Supplemental Figure 2. Wild type and mutant SypE protein expression**. Protein expression of wild type SypE and mutant derivatives was assessed by Western blot analysis. FLAG epitope fusions were generated to the C-terminus of the indicated SypE proteins. Plasmids expressing FLAG-*sypE* alleles were introduced into *sypE* strain containing *rscS* plasmid (pARM7). Samples were prepared as described in Materials and Methods. (A) Expression of SypE truncation mutants. (1) $SypE^{NTD}$, (2) $SypE^{NTD, N52A}$, (3) $SypE^{CTD}$ (4) $SypE^{CTD, D443A}$, (5) $SypE^{CTD, D495A}$. (B) Expression of WT SypE and SypE single point mutants. (1) WT $SypE^{+}$, (2) $SypE^{D192A}$, (3) $SypE^{D443A}$, (4) $SypE^{D495A}$, or (5) untagged WT $SypE^{+}$. (C) Expression of SypE double point mutants. (1) WT $SypE^{+}$, (2) $SypE^{N52A}$, (3) $SypE^{N52A, D192A}$, (4) $SypE^{N52A, D443A}$, (5) $SypE^{N52A, D495A}$

# Morris *et al.*, Supplemental Figure 3

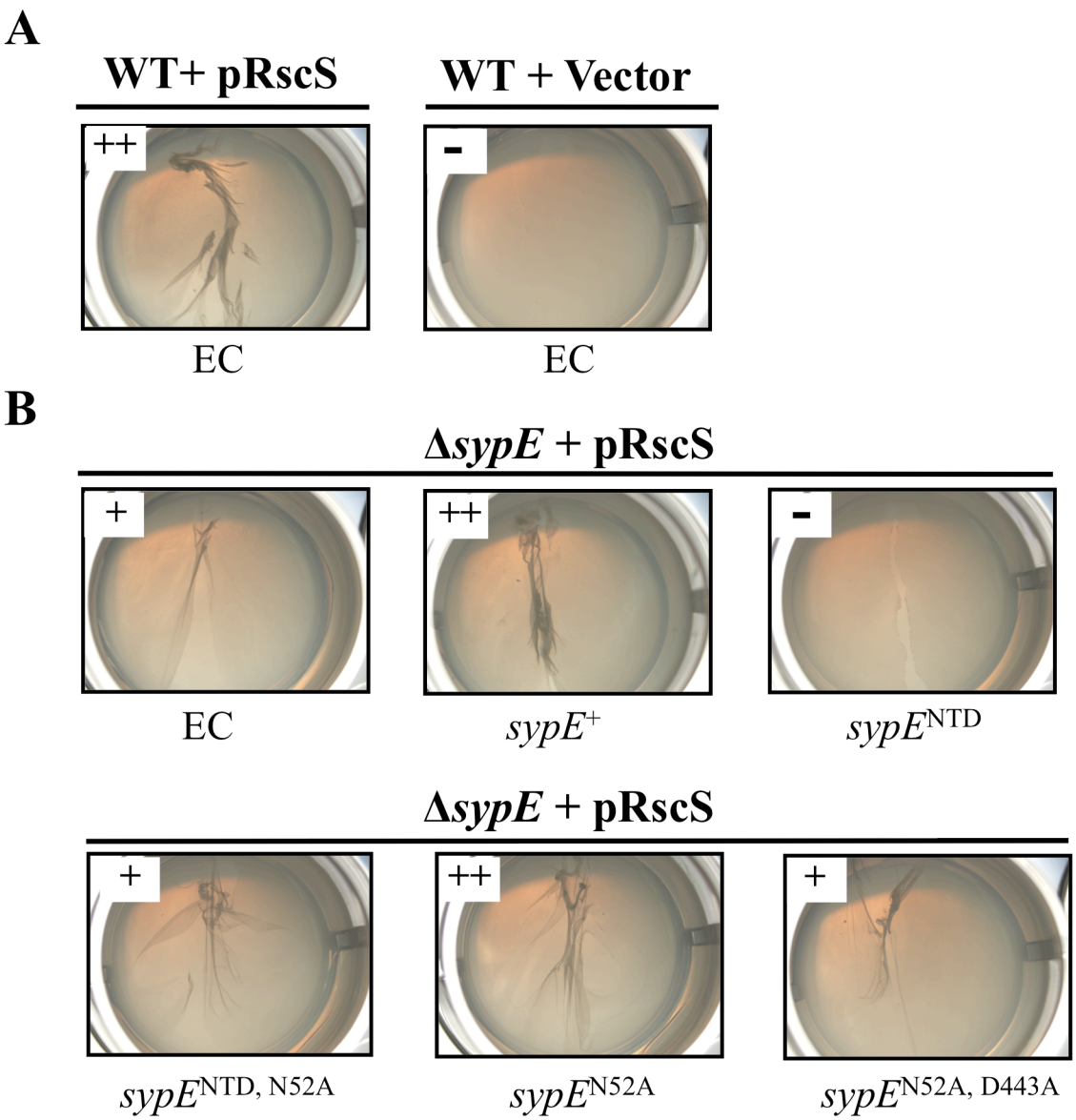


**Supplemental Figure 3. SypE N-terminal domain inhibits RscS-induced pellicles.** Pellicle formation assay of RscS-expressing strains. Strains were cultured in HMM at RT and pellicle formation assessed at 48 h post inoculation. (A) Wild-type cells containing empty Tn*7* cassette (EC) and carrying either pRscS plasmid (pARM7) or vector control (pKV282). (B) pARM7 in Δ*sypE* cells complemented with: empty cassette [KV4390], WT *sypE*$^{+}$ [KV4819], *sypE*$^{NTD}$ [KV5129], *sypE*$^{NTD, N52A}$ [KV5143], *sypE*$^{N52A}$ [KV5142], *sypE*$^{N52A, D443A}$ [KV5379]. A pipette tip was dragged over the surface of the air-liquid interface to visualize the pellicle. Relative pellicle strength was determined as described in supplemental Figure 1.

**Morris *et al.*, Supplemental Figure 4**

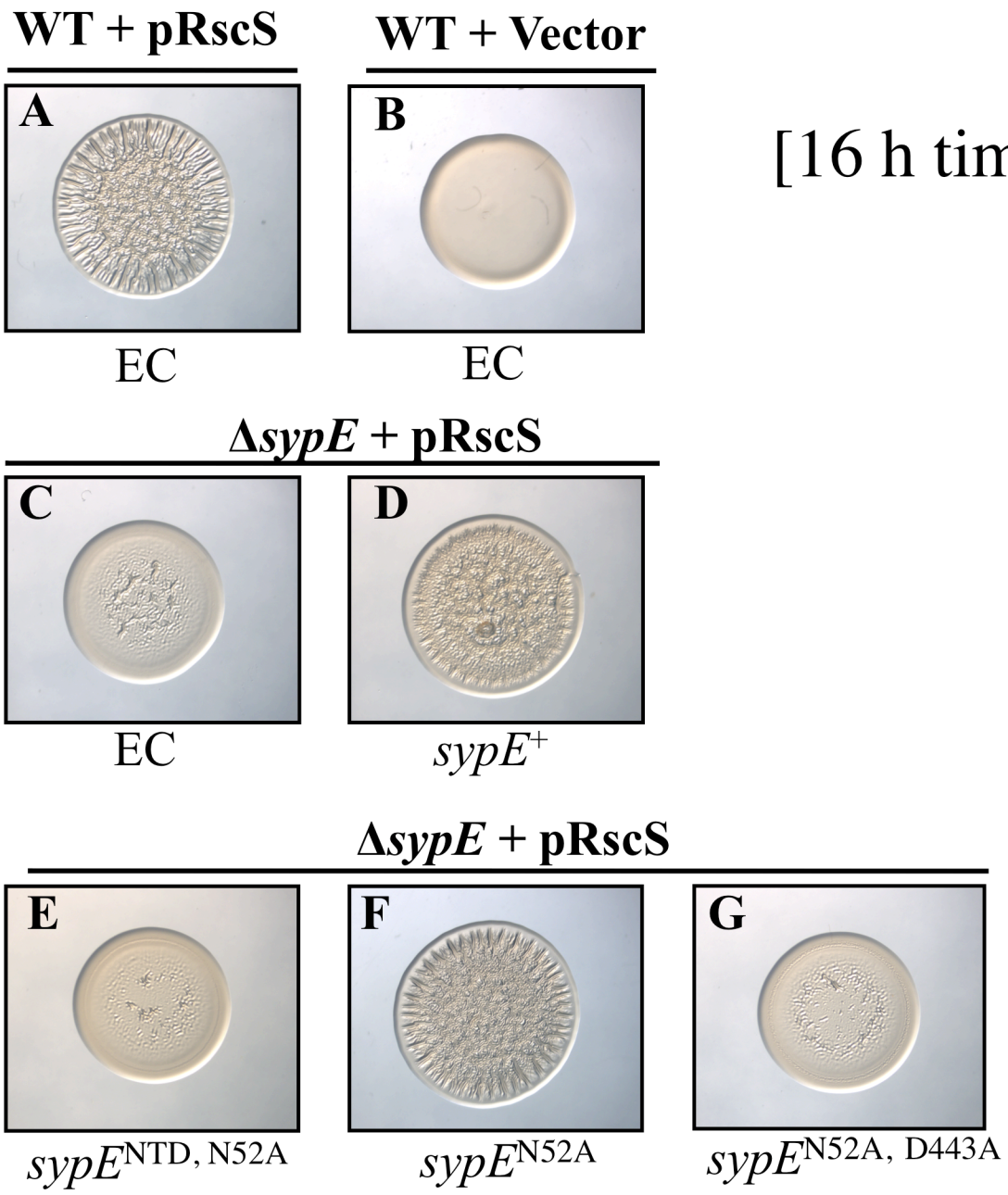


**Supplemental Figure 4. SypE-mediated positive regulation of RscS biofilms.** Wrinkled colony assay of RscS-induced biofilm. Strains were spotted onto LBS media at RT and wrinkled colony formation assessed at an early time point (16h post-spotting). WT ES114 containing empty Tn*7* cassette (EC) (KV4389) and carrying RscS plasmid pARM7 (A) or vector control pKV282 (B); pARM7 in Δ*sypE* cells complemented with*:* (C) EC [KV4390], (D) WT *sypE*$^{+}$ [KV4819], (E) *sypE*$^{\text{NTD, N52A}}$ [KV5143], (F) *sypE*$^{\text{N52A}}$ [KV5142], (G) *sypE*$^{\text{N52, D443A}}$ [KV5379].

# Morris *et al.*, Supplemental Figure 5

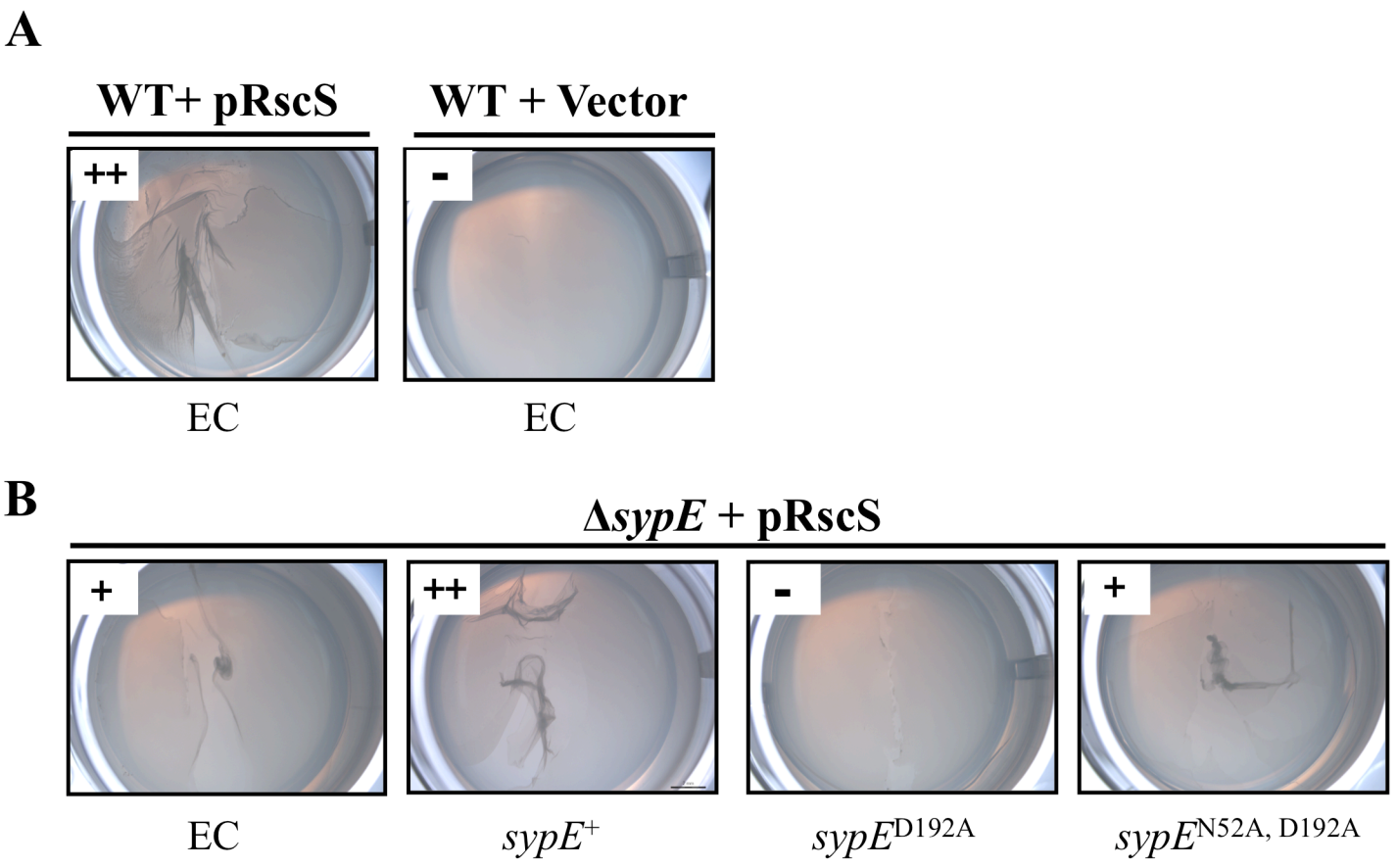


**Supplemental Figure 5. SypE central REC domain regulates SypE activity.** Pellicle formation assay of RscS-expressing strains. Strains were cultured in HMM at RT and pellicle formation assessed at 48 h post inoculation. (A) Wild-type cells containing empty Tn*7* cassette (EC) and carrying either pRscS plasmid (pARM7) or vector control (pKV282). (B) pARM7 in Δ*sypE* cells complemented with: empty cassette [KV4390], WT *sypE*$^{+}$ [KV4819], *sypE*$^{D192A}$ [KV4885], *sypE*$^{N52A, D192A}$ [KV5205]. A pipette tip was dragged over the surface of the air-liquid interface to visualize the pellicle. Relative pellicle strength was determined as described in supplemental Figure 1.